Published for SISSA by Springer

Received: December 16, 2021
Accepted: February 16, 2022
Published: March 3, 2022

Large charges on the Wilson loop in $\mathcal{N} = 4$ SYM: matrix model and classical string

Simone Giombi,[a] **Shota Komatsu**[b] **and Bendeguz Offertaler**[a]

[a] *Joseph Henry Laboratories, Princeton University, Princeton, NJ 08544, U.S.A.*
[b] *Department of Theoretical Physics, CERN, 1211 Meyrin, Switzerland*

E-mail: sgiombi@princeton.edu, shota.komadze@gmail.com, bendeguz@princeton.edu

Abstract: We study the large charge sector of the defect CFT defined by the half-BPS Wilson loop in planar $\mathcal{N} = 4$ supersymmetric Yang-Mills theory. Specifically, we consider correlation functions of two large charge insertions and several light insertions in the double-scaling limit where the 't Hooft coupling λ and the large charge J are sent to infinity, with the ratio $J/\sqrt{\lambda}$ held fixed. They are holographically dual to the expectation values of light vertex operators on a classical string solution with large angular momentum, which we evaluate in the leading large J limit. We also compute the two-point function of large charge insertions by evaluating the on-shell string action, supplemented by the boundary terms that generalize the one introduced by Drukker, Gross and Ooguri for the Wilson loop without insertions. For a special class of correlation functions, we reproduce the string results from field theory by using supersymmetric localization. The results are given by correlation functions in an "emergent" matrix model whose matrix size is proportional to J and whose spectral curve coincides with that of the classical string. Similar matrix models appeared in the study of extremal correlators in rank-1 $\mathcal{N} = 2$ superconformal field theories, but our results hold also for non-extremal cases.

Keywords: AdS-CFT Correspondence, Matrix Models, Wilson, 't Hooft and Polyakov loops

ArXiv ePrint: 2110.13126

https://doi.org/10.1007/JHEP03(2022)020

JHEP03(2022)020

Contents

JHEP03(2022)020

1 Introduction and summary

The study of operators with large quantum numbers has played a central role in the development of the gauge/string duality and AdS/CFT correspondence [1, 2]. Under the duality, operators with large quantum numbers are dual to macroscopic string states, which can be quantized by semiclassical methods. For instance, the scaling dimensions of single-trace operators with large charges in the gauge theory are dual to the energies of semiclassical closed string states in AdS. The investigation of such large charge sectors of AdS/CFT also paved the way to the discovery of integrable structures on the gauge and string sides, leading to rather non-trivial dynamical tests of the correspondence (see for instance [3] for a review of this extensive topic). More recently, general properties of the large charge expansion in CFTs with global symmetries have been extensively studied using effective field theory methods, see for instance [4–7] and [8] for a recent review.

In this work, our focus is on the large charge sector of the defect CFT associated with the half-BPS Wilson loop in the $\mathcal{N} = 4$ supersymmetric Yang-Mills (SYM) theory. This is a well-known generalization of the usual Wilson loop operator that couples to one of the scalar fields of the theory, and is supported on a circular (or infinite straight line) contour. It preserves a one-dimensional superconformal group $\mathrm{OSp}(4^*|4)$ that includes 16 supercharges (half of the superconformal symmetry of the $\mathcal{N} = 4$ SYM theory) and the bosonic subgroup

$\mathrm{SL}(2,\mathbb{R}) \times \mathrm{SO}(3) \times \mathrm{SO}(5)$. Here $\mathrm{SL}(2,\mathbb{R})$ is the 1d conformal symmetry preserved by a circle (or line), $\mathrm{SO}(3)$ is the symmetry under spacetime rotations transverse to the defect, and $\mathrm{SO}(5)$ is the residual R-symmetry that rotates the five scalars that do not couple to the Wilson loop. The correlation functions of operator insertions on the Wilson loop (together with correlation functions involving "bulk" single-trace operators) define a rather rich defect CFT that is amenable to studies via holography [9–11], localization [11–13], conformal bootstrap [14–16] and integrability [9, 17–21].[1]

A Wilson loop operator in the fundamental representation is dual to an open string minimal surface extending in AdS and ending at the boundary on the contour that defines the loop operator. For the half-BPS Wilson loop, the corresponding minimal surface is an open string worldsheet with AdS_2 induced geometry. Defect operator insertions on the Wilson loop are dual to fluctuations of the string about the AdS_2 geometry, and their correlation functions at strong coupling can be computed holographically by evaluating Witten diagrams in the string sigma model perturbation theory. For instance, the 4-point functions of the "elementary" insertions dual to fluctuations of string coordinates in static gauge were computed in [10]. Similarly, one can also compute correlation functions of "composites" of those excitations (see for instance [12] for some explicit examples). This perturbative approach via AdS_2 Witten diagrams is appropriate as long as the quantum numbers of the inserted operators are small compared to the string tension, or $\sqrt{\lambda}$ (where $\lambda = g_{\mathrm{YM}}^2 N$ is the gauge theory 't Hooft coupling, and in this paper we focus on the planar limit throughout). When the quantum numbers become of order $\sqrt{\lambda}$, the boundary insertions are of the same order as the string action and one then expects a new open string solution to dominate the path-integral. A special class of operator insertions that are ideal for exploring this regime are the chiral primaries corresponding to products of scalar fields transforming in the symmetric traceless representations of the $\mathrm{SO}(5)$ R-symmetry. These operators have protected scaling dimensions, but their two-point and three-point functions are non-trivial functions of the coupling constant that can nevertheless be computed exactly via localization [12, 13]. More generally, localization allows to compute the n-point functions in a subsector of "topological" chiral primaries (to be reviewed below), which have position independent correlation functions.

In the large charge regime, the simplest object to consider in the defect CFT is the insertion of two chiral primaries with charge J such that

$$J \to \infty\,, \quad \lambda \to \infty\,, \quad \frac{J}{\sqrt{\lambda}} \ \text{fixed}\,. \tag{1.1}$$

On the string theory side, the worldsheet corresponding to this configuration was identified first in [9] in the limit $\frac{J}{\sqrt{\lambda}} \to \infty$, and later generalized to finite $\frac{J}{\sqrt{\lambda}}$ in [28].[2] We review the solution in detail in section 4. Starting from this string worldsheet and inserting additional operators with small quantum numbers, one can then obtain new results on correlation

[1] The defect CFT defined by the half-BPS Wilson loop is also of interest in the study of renormalization group flows on defects. It can be thought as the IR fixed point of a RG flow which starts in the UV from the ordinary, non-supersymmetric Wilson loop [22–24]. See also [25–27] for related work.

[2] In [28] a general solution parametrized by two cusp angles was considered. Here we focus on the case where both angles are zero, which corresponds to insertions on a straight line or circular loop.

JHEP03(2022)020

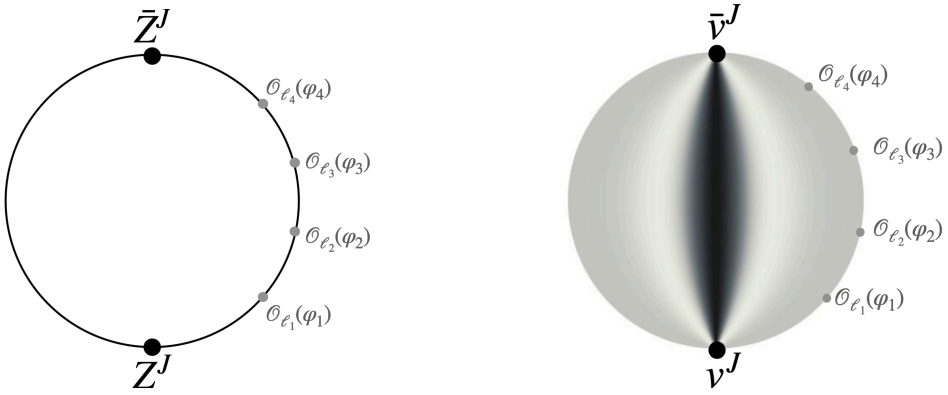

a. $\mathcal{N} = 4$ SYM **b.** String

Figure 1. Large charge correlation functions on the gauge theory side and on the string theory side. **a.** Correlation functions of insertions on the half-BPS circular Wilson loop. In this paper, we take two of them (Z^J and $\bar{Z}^J$) to have large charges ($J \sim \sqrt{\lambda} \gg 1$) and the others ($\mathcal{O}_{\ell_j}(\varphi_j)$'s) to be light. **b.** At strong coupling, the same correlation functions are described by a non-trivial classical string solution which ends at the Wilson loop on the boundary. In the absence of the insertions, the string worldsheet lies on the Euclidean AdS_2 subspace inside $AdS_5 \times S^5$. The large charge insertions deform this solution and the string worldsheet has a non-trivial profile around the insertion points. As an illustration of the string solution, the figure above shows a density plot of the worldsheet curvature. The leading large J answer can be computed by evaluating the light vertex operators on this deformed solution.

functions of two "heavy" (large charge) operators and any number of "light" operators, normalized by the heavy-heavy two-point function. See figure 1. These correlators include in particular the defect CFT OPE data in the heavy-heavy-light configuration. In this paper we focus on the leading order in the large charge limit (1.1), corresponding to the classical analysis on the string side, while subleading corrections corresponding to quantum fluctuations will be discussed in the companion paper [29].

A more basic quantity that one can also study is the correlation function of the two heavy operators alone. Since the operators are protected with dimension $\Delta = J$, their two-point function on the Wilson loop has the form

$$\langle O_J O_J \rangle = \frac{n_J(\lambda)}{d^{2J}}, \tag{1.2}$$

where d is the distance between the operators, and $n_J(\lambda)$ is a non-trivial function of the coupling constant and charge J. This normalization constant has physical meaning because the operators are protected (for instance, for $J = 1$ it is related to the Bremsstrahlung function [18]). In the large charge limit, eq. (1.1), it is expected to exponentiate as $n_J(\lambda) \sim e^{\sqrt{\lambda} f(J/\sqrt{\lambda})}$, where the non-trivial function in the exponent should correspond to the classical string action. In section 4 we discuss this holographic two-point calculation in detail (refining and extending earlier attempts in [30]). We will propose, in particular, that a suitable modification of the boundary term prescription of [31] is needed in this case to properly account for the presence of the boundary vertex operators for the large charge insertions.

JHEP03(2022)020

A non-trivial test of the string theory predictions can be obtained by comparing to the localization approach, which was developed in [12, 13] in the present context of the defect CFT on the Wilson loop. Interestingly, when two chiral primaries with semiclassical charges $J \sim \sqrt{\lambda}$ are inserted, the localization results can be recast in terms of the "planar" limit of a matrix model of a $J \times J$ Hermitean matrix.[3] Using this matrix model description, in section 3 we obtain the localization prediction for the two-point function of the heavy operators as well as the topological n-point functions of the two heavy operators and any number of light primaries, working to leading order in the large charge limit. The results are found to be in complete agreement with the string theory predictions we obtain in section 4. On the string theory side, in addition to the modified boundary term mentioned above, an additional ingredient that is crucial to obtain the correct result for the correlation functions is the averaging over a classical modulus of the string solution— namely, a constant angle ϕ_0 corresponding to the circle on S^5 that is dual to the charge J. This averaging is similar to the one recently advocated in [32], and previously in [33] (see also [5] for the analogous effect in the effective field theory description of the large charge expansion of CFTs).

It is interesting to note that our matrix model shares some features with the matrix model derived in [34], which describes the extremal correlation functions in $\mathcal{N} = 2$ SCFTs. In particular, the size of the matrix in both cases is given by the R-charge of the operators. However, there are also notable differences. Firstly, while the matrix model in [34] describes a subsector of the rank-1 SCFTs[4] e.g. SU(2) $\mathcal{N} = 4$ SYM, our matrix model describes a subsector of U(N) $\mathcal{N} = 4$ SYM at large N, which is in a completely different parameter regime. Secondly, in the setup discussed in [34], all the physical information is in the two-point function,[5] and correspondingly, the matrix model only computes such two-point functions. By contrast, in our setup, there are non-extremal higher-point functions which encode non-trivial physical information, and we can study them using our matrix model. Finally and perhaps most importantly, the classical spectral curve of our matrix model, which controls the leading large charge answer, coincides with the spectral curve of the classical string solution describing the holographic dual of the large charge operators on the Wilson loop. This provides a clear physical interpretation of the spectral curve of the large charge matrix model [28]. In addition, it suggests that the structure observed in the topological subsector may extend to more general non-SUSY sectors. This optimism comes from the fact that the spectral curve of the classical string is known to control the full non-protected spectrum of semiclassical fluctuations on the worldsheet [36, 37].

There are several future directions worth exploring. First, it would be interesting to consider large charge limits of the correlation functions which involve "bulk operators", namely operators outside the defect (previous work on some of these observables include [38–40]). Studying such correlation functions would allow us to analyze the interplay between the large charge limit and the defect crossing equation. Second, the generalization of our

[3] This matrix model was obtained first in [28] using integrability-based methods, and was rederived in [12] using the localization approach.

[4] The generalization of [34] to higher-rank theories was discussed in [35].

[5] This is because all the other extremal correlation functions, including the three-point functions, are automatically determined by the normalization of the two-point function.

JHEP03(2022)020

results to 1/8-BPS Wilson loops [41–43] should be possible. In this case, the relation to the defect CFT will be lost since general 1/8-BPS Wilson loops do not preserve the conformal symmetry. Nevertheless, we can analyze the correlation functions on these Wilson loops both from the localization and the (semi-)classical string. Third, the localization analysis can be applied away from the large N limit, in particular to SU(2) $\mathcal{N}=4$ SYM [12]. The large charge limit in this case would be more directly related to large charge limits of rank-1 SCFTs studied in the literature [34, 44], and it would be interesting to explore their relation.

The remainder of this paper is organized as follows. In section 2 we review some basic facts about the defect CFT on the half-BPS Wilson loop and introduce the large charge operators of interest in this paper. In section 3 we review the localization results for the correlation functions on the Wilson loop and the matrix model describing the large charge sector, and then use it to compute the two-point function of the heavy operators and the topological n-point functions of two heavy and any number of light operators. In section 4 we introduce the string solution describing the insertion of two large charges on the Wilson loop, and then discuss the computation of the two-point function of the heavy operators and the correlation functions of the two heavy and any number of light operators. The appendices include some technical details on the "quasi-momentum" associated to the matrix model and on the supersymmetries preserved by the string solution.

2 Large charges in the Wilson loop defect CFT

This section introduces the defect CFT observables we will analyze in this paper. First, our conventions for $\mathcal{N}=4$ SYM: we work in Euclidean signature and use the standard Cartesian coordinates x^μ, $\mu=1,\dots,4$, on $\mathbb{R}^4$. We take the gauge group to be U(N), denote the Yang-Mills coupling constant $g_{\rm YM}$, and the 't Hooft coupling $\lambda\equiv g_{\rm YM}^2 N$. Below we will also often adopt the notation $g\equiv\frac{\sqrt{\lambda}}{4\pi}$ commonly used in the integrability literature.

The Wilson loop defect CFT. Our starting point is the half-BPS Wilson loop in $\mathcal{N}=4$ SYM whose contour is a circle and which couples to a single scalar. The Wilson loop is

$$\mathcal{W}\equiv\frac{1}{N}\mathrm{Tr\ P\ exp}\left(\oint\left(iA_\mu(x)\dot{x}^\mu+|\dot{x}|\Phi_6(x)\right)d\varphi\right)\,, \tag{2.1}$$

where $\dot{x}^\mu=\frac{dx^\mu}{d\varphi}$ and φ is a coordinate parameterizing the loop. Below we will mostly work with the explicit parameterization $x^\mu(\varphi)=(\cos\varphi,\sin\varphi,0,0)$ with $\varphi\in[-\pi,\pi)$ (in which case $|\dot{x}|=1$). The gauge field A_μ and the scalars Φ_I, $I=1,\dots,6$, transform in the adjoint of U(N) and the trace is taken in the fundamental. The expectation value of $\mathcal{W}$, as well as its planar limit ($N\to\infty$, g fixed) and supergravity limit ($N\to\infty$, $g\gg1$), is well known [45–47]:

$$\langle\mathcal{W}\rangle_{\mathcal{N}=4\ \mathrm{SYM}}=\frac{1}{N}L_{N-1}^1\left(-\frac{g_{\rm YM}^2}{4}\right)e^{\frac{g_{\rm YM}^2}{8}}\overset{N\to\infty}{\to}\frac{1}{2\pi g}I_1(4\pi g)\overset{g\gg1}{\sim}\frac{e^{4\pi g}}{4\sqrt{2}\pi^2 g^{3/2}}. \tag{2.2}$$

The Wilson loop preserves an SL($2,\mathbb{R}$) subgroup of the SO(5,1) conformal group of $\mathcal{N}=4$ SYM and defines a one dimensional defect CFT in which local adjoint operators

JHEP03(2022)020

$O_i(x)$, $i = 1, \ldots, n$ are inserted along the contour [9–15, 19–21, 23, 24, 48, 49]. We will use the "single bracket" notation for the unnormalized defect correlators given by

$$\langle O_1(\varphi_1) \ldots O_n(\varphi_n) \rangle \equiv \left\langle \frac{1}{N} \mathrm{Tr\ P} \left[O_1(\varphi_1) \ldots O_n(\varphi_n) e^{\int (iA_\mu \dot{x}^\mu + \Phi_6) d\varphi} \right] \right\rangle_{\mathcal{N}=4 \text{ SYM}}, \tag{2.3}$$

where $O_i(\varphi_i) \equiv O_i(x(\varphi_i))$ and the path ordering in the $\mathcal{N} = 4$ SYM correlator acts both on the local operators and on the Wilson loop. It is also convenient to define the "double bracket" defect correlators normalized by the Wilson loop expectation value

$$\langle\langle O_1(\varphi_1) \ldots O_n(\varphi_n) \rangle\rangle \equiv \frac{\langle O_1(\varphi_1) \ldots O_n(\varphi_n) \rangle}{\langle \mathcal{W} \rangle_{\mathcal{N}=4 \text{ SYM}}}, \tag{2.4}$$

which satisfy $\langle\langle 1 \rangle\rangle = 1$. The defect correlators obey the axioms outlined in appendix A of [50] for correlators in a one dimensional CFT. Since the defect is a circle, the conformal correlators are composed of ratios of the chordal distances, which we will denote

$$d_{ij} \equiv d(\varphi_i, \varphi_j) \equiv 2 \sin \left(\frac{\varphi_i - \varphi_j}{2} \right). \tag{2.5}$$

Although our discussion is framed in terms of the circular Wilson loop, the analysis of the half-BPS Wilson line $\mathcal{W}_{\text{line}}$ is essentially equivalent.[6] Its expectation value, $\langle \mathcal{W}_{\text{line}} \rangle_{\mathcal{N}=4 \text{ SYM}} = 1$, differs from eq. (2.2) due to a "conformal anomaly" [45, 46], but the defect correlators on the circle and line, when normalized by the corresponding Wilson loop operator without insertions, behave in the standard way under conformal transformations. Specifically, under the map $t_i = \tan \frac{\varphi_i}{2}$, the correlators are related by

$$\begin{aligned} \frac{\langle O_1(t_1) \ldots O_n(t_n) \mathcal{W}_{\text{line}} \rangle_{\mathcal{N}=4 \text{ SYM}}}{\langle \mathcal{W}_{\text{line}} \rangle_{\mathcal{N}=4 \text{ SYM}}} &= \left(\frac{d \tan \frac{\varphi_1}{2}}{d\varphi_1} \right)^{-\Delta_1} \ldots \left(\frac{d \tan \frac{\varphi_n}{2}}{d\varphi_n} \right)^{-\Delta_n} \langle\langle O_1(\varphi_1) \ldots O_n(\varphi_n) \rangle\rangle \\ &= \langle\langle O_1(\varphi_1) \ldots O_n(\varphi_n) \rangle\rangle \big|_{d_{ij} \to t_{ij}}, \end{aligned} \tag{2.6}$$

where $t_{ij} \equiv t_i - t_j$. Thus, we may readily switch between correlators on the circle and correlators on the line by exchanging chordal distances with Euclidean distances.

Chiral primaries. We are interested in the large charge sector of defect correlators of chiral primaries of the form

$$\mathcal{O}_J(\varphi, \epsilon) \equiv (\epsilon \cdot \Phi(x(\varphi)))^J, \tag{2.7}$$

where $\Phi = (\Phi_1, \ldots, \Phi_5)$ is a vector of the scalar fields not coupled to the Wilson loop in eq. (2.1) and $\epsilon = (\epsilon_1, \ldots, \epsilon_5)$ is a complex polarization vector satisfying $\epsilon^2 = 0$. These operators transform in the symmetric traceless representation of $\mathrm{SO}(5) \subset \mathrm{SO}(6)$ and have protected dimension $\Delta = J$ equal to the R-charge. Conformal symmetry and R-symmetry

[6] One way to explicitly parametrize the half-BPS line is to pick the contour $x^\mu(t) = (t, 0, 0, 0)$ and let

$$\mathcal{W}_{\text{line}} \equiv \frac{1}{N} \mathrm{Tr\ P} \exp \left(\int_{-\infty}^{\infty} (iA_1(x) + \Phi_6(x))\, dt \right).$$

JHEP03(2022)020

then fix the two and three-point functions of the chiral primaries, up to the operator normalizations and OPE coefficients:

$$\langle\langle \mathcal{O}_{J_1}(\varphi_1,\epsilon_1)\mathcal{O}_{J_2}(\varphi_2,\epsilon_2)\rangle\rangle = n_{J_1}(g,N)\frac{(\epsilon_1\cdot\epsilon_2)^{J_1}}{d_{21}^{2J}}\delta_{J_1J_2}, \tag{2.8}$$

$$\langle\langle \mathcal{O}_{J_1}(\varphi_1,\epsilon_1)\mathcal{O}_{J_2}(\varphi_2,\epsilon_2)\mathcal{O}_{J_3}(\varphi_3,\epsilon_3)\rangle\rangle = c_{J_1J_2J_3}(g,N)\frac{(\epsilon_1\cdot\epsilon_2)^{J_{12|3}}(\epsilon_2\cdot\epsilon_3)^{J_{23|1}}(\epsilon_3\cdot\epsilon_1)^{J_{31|2}}}{d_{21}^{2J_{12|3}}d_{32}^{2J_{23|1}}d_{31}^{2J_{31|2}}}. \tag{2.9}$$

Here, $J_{ij|k}\equiv(J_i+J_j-J_k)/2$. The 3-pt function is zero unless J_1, J_2 and J_3 satisfy the triangle inequality ($J_1+J_2\geq J_3$, plus permutations) and sum to an even integer.

Furthermore, the chiral primaries have a topological sector, which is accessible for finite N and g using localization [12], in which the correlators are position independent and the OPE is closed. We will discuss the topological sector in greater detail in section 3, but we presently define the topological operators to be chiral primaries whose polarization vectors are correlated with their positions in the following way:[7]

$$\tilde{\Phi}^J(\varphi)\equiv(\cos\varphi\Phi_3(\varphi)-\sin\varphi\Phi_4(\varphi)+i\Phi_5(\varphi))^J. \tag{2.10}$$

We will usually drop the explicit dependence on φ. Since $\epsilon(\varphi_i)\cdot\epsilon(\varphi_j)=-\frac{1}{2}d_{ij}^2$, the topological two and three-point correlators are manifestly constant:

$$\langle\langle\tilde{\Phi}^{J_1}\tilde{\Phi}^{J_2}\rangle\rangle = \left(-\frac{1}{2}\right)^{J_1} n_{J_1}\delta_{J_1J_2}, \tag{2.11}$$

$$\langle\langle\tilde{\Phi}^{J_1}\tilde{\Phi}^{J_2}\tilde{\Phi}^{J_3}\rangle\rangle = \left(-\frac{1}{2}\right)^{\frac{J_1+J_2+J_3}{2}} c_{J_1J_2J_3}. \tag{2.12}$$

In accordance with localization, higher-point correlators are also constant. Given eqs. (2.8)–(2.9), the topological two and three-point functions fully determine the general two and three-point functions, but the same is not true of the higher-point functions because their form is not fixed up to an overall constant by conformal symmetry.

Correlators in the large charge sector. In this work, we study the correlators of $2+n$ chiral primaries, two of which have charge J and n of which have charges $\ell_1,\ldots,\ell_n$. We analyze the correlators in the *large charge regime*, in which we first take $N\to\infty$ with g, J, and ℓ_i held fixed, and then take $g\to\infty$ with ℓ_i and

$$\mathcal{J}\equiv\frac{J}{g}, \tag{2.13}$$

held fixed. Thus, in the planar limit and strongly coupled regime, the two operators with charge J are the same size as the coupling and the operators with charges ℓ_i are parametrically smaller. We call the former "large charges" or "heavy operators" and the latter "finite charges" or "light operators." In the present work we focus mostly on the leading behavior, and postpone the analysis of subleading corrections in $1/g$ to [29].

[7] This particular definition for the topological operators is equivalent to the one in [12] up to relabelling of scalar flavor indices and flipping the sign of Φ_4.

JHEP03(2022)020

In the first half of our analysis, in section 3, we start from the planar-exact integral representation of the topological correlators that was derived in [12], and use it to derive a matrix model that describes the large charge sector. This lets us determine, to leading order, the normalized higher-point correlators

$$\frac{\langle\langle \tilde{\Phi}^J \tilde{\Phi}^J \prod_{i=1}^n \tilde{\Phi}^{\ell_i} \rangle\rangle}{\langle\langle \tilde{\Phi}^J \tilde{\Phi}^J \rangle\rangle}, \tag{2.14}$$

as well as the two-point function

$$\langle\langle \tilde{\Phi}^J \tilde{\Phi}^J \rangle\rangle. \tag{2.15}$$

In the second half of our analysis, in section 4, we analyze the string dual to the large charge defect correlator

$$\langle\langle Z^J(-\varphi_L) \bar{Z}^J(\varphi_L) \rangle\rangle = \frac{2^J n_J}{d^{2J}}, \tag{2.16}$$

where we have chosen the specific chiral primaries

$$Z \equiv \Phi_4 + i\Phi_5, \qquad \text{and} \qquad \bar{Z} \equiv \Phi_4 - i\Phi_5, \tag{2.17}$$

and where

$$d \equiv d(-\varphi_L, \varphi_L) \tag{2.18}$$

is the chordal distance between the large charges. In eq. (2.16), we have used the rotational symmetry to put the two heavy operators at $\varphi = \pm\varphi_L$ and assume for simplicity that $\varphi_L \in (0, \pi/2]$, but otherwise let the locations of the insertions be general.[8] By evaluating the action and vertex operators of the classical string, we can determine the leading behavior of the two-point function, eq. (2.16), and of higher correlators with additional insertions of powers of Z and $\bar{Z}$. Finally, we will also be able to use the classical string to reproduce the topological correlators computed by the matrix model. This is because Z^J and $\bar{Z}^J$ become topological in the antipodal configuration $\varphi_L = \pi/2$, since

$$Z^J\left(-\frac{\pi}{2}\right) = \tilde{\Phi}^J\left(-\frac{\pi}{2}\right), \qquad \bar{Z}^J\left(\frac{\pi}{2}\right) = (-1)^J \tilde{\Phi}^J\left(\frac{\pi}{2}\right), \tag{2.19}$$

and because the light topological operators, $\tilde{\Phi}^\ell$, truncate to linear combinations of powers of Z and $\bar{Z}$ at leading order.

3 Large charge correlators from localization

In this section, we compute correlation functions with large charge insertions in the topological sector. We achieve this by deriving a matrix model that describes the large charge topological sector and applying the matrix model techniques. We will later see in section 4 that the results obtained from localization are in perfect agreement with the results from the classical string.

[8] Because of the conformal symmetry, we could without loss of generality set $\varphi_L = \pi/2$. However, we prefer to keep φ_L general in order to explicitly keep track of the conformal form of the correlators.

JHEP03(2022)020

3.1 Matrix model for large charge correlators

Integral representation for the topological sector. Let us first review the integral representation of the correlation functions of insertions on the half-BPS Wilson loop in $\mathcal{N}=4$ SYM that was derived in [12, 13].

The correlation functions in the topological sector on the half-BPS Wilson loop at large N are given by the following integral,

$$\langle \prod_{k=1}^{n} \tilde{\Phi}^{L_k} \rangle = \oint d\mu \prod_{k=1}^{n} Q_{L_k}(x)\,, \tag{3.1}$$

where $\tilde{\Phi}^L$ is the charge L protected topological insertion defined in eq. (2.10), $d\mu$ is the measure

$$d\mu = \frac{1}{4\pi g}\frac{dx(x+x^{-1})}{2\pi i x} e^{2\pi g(x+x^{-1})}\,, \tag{3.2}$$

and the contour goes counterclockwise once around the origin. We should emphasize that the l.h.s. of eq. (3.1) is a single bracket correlator, as defined in eq. (2.3).

The functions denoted by Q_{L_k} are called *Q-functions* and are characterized by the following two important properties:

1. They are orthogonal under the measure $d\mu$:

$$\oint d\mu\, Q_J(x) Q_M(x) \propto \delta_{JM}\,. \tag{3.3}$$

2. They are polynomials in $X \equiv g(x-x^{-1})$ with a unit leading coefficient:

$$Q_J(x) = X^J + \cdots\,. \tag{3.4}$$

These two properties uniquely determine the functions Q_J, and they can be computed systematically by performing the Gram-Schmidt orthogonalization on the set of monomials $\{1, X, X^2, \cdots\}$. Applying the Gram-Schmidt procedure, we obtain the simple expression:

$$Q_J(x) = \frac{1}{D_J}\begin{vmatrix} \mathcal{I}_0 & \mathcal{I}_1 & \cdots & \mathcal{I}_J \\ \mathcal{I}_1 & \mathcal{I}_2 & \cdots & \mathcal{I}_{J+1} \\ \vdots & \vdots & \ddots & \vdots \\ \mathcal{I}_{J-1} & \mathcal{I}_J & \cdots & \mathcal{I}_{2J-1} \\ 1 & X & \cdots & X^J \end{vmatrix}\,, \tag{3.5}$$

$$D_J \equiv \det\left(\mathcal{I}_{j+k-2}\right)_{1\le j,k\le J} \qquad \mathcal{I}_j \equiv \oint d\mu \left(g(x-x^{-1})\right)^j\,. \tag{3.6}$$

One important identity that follows from the orthogonalization is the expression for the two-point function

$$\langle \tilde{\Phi}^J \tilde{\Phi}^M \rangle = \oint d\mu\; Q_J(x) Q_M(x) = \frac{D_{J+1}}{D_J}\delta_{JM}\,. \tag{3.7}$$

The relations, eq. (3.5) and eq. (3.7), hold for any choice of the measure $d\mu$ as long as the Q's satisfy the aforementioned two properties. This will be important in the analysis of higher-point functions, as we will see shortly.

JHEP03(2022)020

Matrix model. Another identity that we use in this section is the matrix model expression for the determinant D_J. This can be derived by expanding the determinant and expressing each component as an integral (see section 7 of [12]). The result reads

$$D_J = \frac{g^{J(J-1)}}{J!}\left(\prod_{k=1}^{J}\oint d\mu(x_k)\right)\prod_{i<j}(x_i-x_j)^2\left(1+\frac{1}{x_i x_j}\right)^2 . \tag{3.8}$$

Alternatively we can write it in terms of $X_k \equiv g(x_k - x_k^{-1})$ as[9]

$$D_J = \frac{1}{J!}\left(\prod_{k=1}^{J}\oint \underbrace{\frac{dX_k}{8g^2\pi^2 i}e^{2\pi\sqrt{X_k^2+4g^2}}}_{=d\mu(x_k)}\right)\prod_{i<j}(X_i-X_j)^2 , \tag{3.9}$$

where the integration contours are around the branch cut of $\sqrt{X_k^2+4g^2}$. Setting aside the unusual choice of contour, this can be regarded as the eigenvalue integral for the partition function of a $J\times J$ Hermitian matrix model with potential $e^{2\pi\sqrt{M^2+4g^2}}/(8g^2\pi^2 i)$:

$$D_J = \frac{Z_J}{J!} \qquad \text{with} \qquad Z_J \equiv \oint [dM]\frac{e^{2\pi\sqrt{M^2+4g^2}}}{8g^2\pi^2 i} . \tag{3.10}$$

We can also express the two-point function, eq. (3.7), directly in terms of this matrix model. For this purpose, we first rewrite D_{J+1} as

$$D_{J+1} = \frac{1}{(J+1)!}\left(\oint\frac{dY}{8g^2\pi^2 i}e^{2\pi\sqrt{Y^2+4g^2}}\right)\left[\left(\prod_{k=1}^{J}\oint\frac{dX_k}{8g^2\pi^2 i}e^{2\pi\sqrt{X_k^2+4g^2}}(Y-X_k)^2\right)\prod_{i<j}(X_i-X_j)^2\right].$$

The terms in the square bracket can be identified with the expectation value of the square of the determinant operator in the matrix model, $\det(Y-M)^2$. Dividing this by D_J, we obtain

$$\langle\tilde{\Phi}^J\tilde{\Phi}^J\rangle = \frac{D_{J+1}}{D_J} = \frac{1}{J+1}\oint d\mu(y)\langle\det(Y-M)^2\rangle_J , \tag{3.11}$$

where $Y\equiv g(y-y^{-1})$ and $\langle\bullet\rangle_J$ denotes the expectation value in the matrix model:

$$\langle f(M)\rangle_J \equiv \frac{1}{Z_J}\oint[dM]\frac{e^{2\pi\sqrt{M^2+4g^2}}}{8g^2\pi^2 i}f(M). \tag{3.12}$$

Let us make several comments about this matrix model. First, eq. (3.8) was derived initially from integrability in [28] in the computation of the generalized cusp anomalous dimension. It was later re-derived in [12] from localization and was shown to control the two-point function in the topological sector as well.

[9] If one instead performs a change of variables $x_i = ie^{i\theta_i}$, the interaction term in eq. (3.8) becomes

$$(x_i-x_j)^2\left(1+\frac{1}{x_i x_j}\right)^2 = -16\sin^2\left(\frac{\theta_i-\theta_j}{2}\right)\sin^2\left(\frac{\theta_i+\theta_j}{2}\right) ,$$

which coincides with the Vandermonde factor for the matrix model of the orthogonal group $\mathrm{SO}(2N)$.

JHEP03(2022)020

Second, it has several similarities with the large-charge matrix model in [34], which computes the extremal correlation functions in rank-1 $\mathcal{N} = 2$ SCFTs. In both cases, the matrix model was derived by applying the Gram-Schmidt orthogonalization to the localization results and the sizes of the matrices are related to the charges of the operators. Note however that the parameter regimes described by the two models are quite different. The matrix model in [34] is for the rank-1 SCFTs, a canonical example being $\mathcal{N} = 4$ SYM with the SU(2) gauge group. By contrast, our matrix model is for the large N limit of $\mathcal{N} = 4$ SYM. Another difference is that our model can be applied to the non-extremal correlation functions, as we will see below.

Third, since the measure is given by $d\mu \sim e^{2\pi g(x+x^{-1})}$ the standard large N limit in the matrix model corresponds to the limit in which J is large but J/g is kept fixed. In terms of the 't Hooft coupling λ, this corresponds to the limit

$$J \sim \sqrt{\lambda} \gg 1\,, \tag{3.13}$$

which is precisely the strong coupling limit in which the theory is described by classical strings. In other words, the large J expansion of the matrix model gives the semi-classical quantization of the classical string.

Higher-point functions. Let us now use the formalism reviewed above to derive a matrix model representation for the correlation functions of two large-charge insertions ($\tilde{\Phi}^J$) and several light insertions ($\tilde{\Phi}^{\ell_k}$):

$$\langle \tilde{\Phi}^J \tilde{\Phi}^J \prod_{j=1}^{n} \tilde{\Phi}^{\ell_j} \rangle = \oint d\mu\, Q_J(x) Q_J(x) \prod_{j=1}^{n} Q_{\ell_j}(x)\,. \tag{3.14}$$

To compute this correlation function, we first deform the measure by exponentiating the light operators:

$$d\tilde{\mu} \equiv d\mu \exp\left[t \prod_{j=1}^{n} Q_{\ell_j}(x) \right]\,. \tag{3.15}$$

Next, we construct the orthogonal polynomials of X under this measure, which we denote by $\tilde{Q}_J(x,t)$. Using the relations reviewed in the previous section, we can express the two-point function of the $\tilde{Q}_J$'s as a ratio of (deformed) determinants,

$$\oint d\tilde{\mu}\ \tilde{Q}_J(x,t)\tilde{Q}_J(x,t) = \frac{\tilde{D}_{J+1}}{\tilde{D}_J}\,, \tag{3.16}$$

with

$$\tilde{D}_J \equiv \det\left(\tilde{\mathcal{I}}_{j+k-2}\right)_{1\le j,k\le J}\,, \qquad \tilde{\mathcal{I}}_j \equiv \oint d\tilde{\mu}\left(g(x-x^{-1})\right)^j\,. \tag{3.17}$$

Then we differentiate the left hand side of eq. (3.16) with respect to t and set t to zero. Since both the measure and $\tilde{Q}$ depend on t, the differentiation produces three different terms,

$$\oint d\mu\, Q_J(x) Q_J(x) \prod_{j=1}^{n} Q_{\ell_j}(x)\,, \qquad \oint d\mu\, \frac{d\tilde{Q}_J}{dt}\bigg|_{t=0} Q_J\,, \qquad \oint d\mu\, Q_J\ \frac{d\tilde{Q}_J}{dt}\bigg|_{t=0}\,. \tag{3.18}$$

JHEP03(2022)020

However, the latter two terms identically vanish for the following reason: since the leading coefficient of the polynomial $\tilde{Q}_J$ is 1, the derivative $d\tilde{Q}_J/dt$ is always a polynomial of lower degree. Thus one can express $d\tilde{Q}_J/dt|_{t=0}$ as a linear combination of Q_M with $M < L$. We can then use the orthogonality of the Q-functions, eq. (3.7), to conclude that the latter two integrals vanish.

In summary, we arrive at the equality

$$\begin{aligned}\langle \Phi^J \Phi^J \prod_{j=1}^{n} \Phi^{\ell_j} \rangle &= \oint d\mu Q_J(x) Q_J(x) \prod_{j=1}^{n} Q_{\ell_j}(x) = \frac{d}{dt}\left[\oint d\tilde{\mu}\ \tilde{Q}_J(x,t)\tilde{Q}_J(x,t)\right]\Big|_{t=0} \\ &= \frac{d}{dt}\frac{\tilde{D}_{J+1}}{\tilde{D}_J}\Big|_{t=0} .\end{aligned} \tag{3.19}$$

If we divide this correlation function by the two-point function of the heavy insertions, we arrive at the simpler formula

$$\frac{\langle \tilde{\Phi}^J \tilde{\Phi}^J \prod_{j=1}^{n} \tilde{\Phi}^{\ell_j} \rangle}{\langle \tilde{\Phi}^J \tilde{\Phi}^J \rangle} = \frac{d \log \tilde{D}_{J+1}}{dt} - \frac{d \log \tilde{D}_J}{dt}\Big|_{t=0} . \tag{3.20}$$

Now the final step is to translate this into the matrix model. As with D_J, the deformed determinant admits a matrix model representation eq. (3.8) with $d\mu$ replaced with $d\tilde{\mu}$. By differentiating it with respect to t and setting it to zero, we get

$$\frac{d\tilde{D}_J}{dt}\Big|_{t=0} = \frac{g^{J(J-1)}}{J!}\left(\prod_{k=1}^{J}\oint d\mu(x_k)\right)\prod_{i<j}(x_i - x_j)^2\left(1+\frac{1}{x_i x_j}\right)^2 \sum_{k=1}^{J}\left(\prod_{j=1}^{n} Q_{\ell_j}(x_k)\right) \tag{3.21}$$

In the matrix model language, after dividing by D_J, this corresponds to the expectation value of the "single-trace operator" $\mathrm{Tr}\left[\prod_{j=1}^{n} Q_{\ell_j}(M)\right]$. Therefore, we arrive at the relation

$$\frac{\langle \tilde{\Phi}^J \tilde{\Phi}^J \prod_{j=1}^{n} \tilde{\Phi}^{\ell_j} \rangle}{\langle \tilde{\Phi}^J \tilde{\Phi}^J \rangle} = \left\langle \mathrm{Tr}\left[\prod_{j=1}^{n} Q_{\ell_j}(M)\right]\right\rangle_{J+1} - \left\langle \mathrm{Tr}\left[\prod_{j=1}^{n} Q_{\ell_j}(M)\right]\right\rangle_{J} . \tag{3.22}$$

Note that this formula naturally reduces to the original integral representation eq. (3.1) when $J = 0$ because $\langle \bullet \rangle_{J=1}$ is a single-integral with the measure $d\mu$, and $\langle \bullet \rangle_{J=0} = 0$.

3.2 Large J analysis

Higher-point functions. To evaluate eq. (3.22) in the large J limit, it is convenient to use the quasi-momentum discussed in [12, 28]:

$$\begin{aligned} p(x) &\equiv \frac{1+x^2}{1-x^2}\sum_{k=1}^{J}\frac{1}{g(x-x^{-1}) - g(x_k - x_k^{-1})} \\ &= \frac{x^2}{g(1-x^2)}\sum_{k=1}^{J}\left(\frac{1}{x-x_k} + \frac{1}{x+\frac{1}{x_k}} - \frac{1}{x}\right) . \end{aligned} \tag{3.23}$$

To motivate this definition, let us consider the one form $p(x)du$, where u is the Zhukovsky variable often used in the integrability literature:

$$u(x) \equiv g\left(x + \frac{1}{x}\right) . \tag{3.24}$$

JHEP03(2022)020

An important property of this one form is that it has poles with residue -1 at $x = x_k$ and $x = -x_k^{-1}$ and poles with residue J at $x = 0$ and $x = \infty$. In addition, it is related to the resolvent in the matrix model that we introduced earlier. Using the standard definition, the resolvent of the matrix model is

$$R(X) \equiv \sum_{k=1}^{J} \frac{1}{X - X_k}\,, \tag{3.25}$$

where we recall that the X_k's are the eigenvalues of the matrix M. Now, by explicit computation, we can check

$$R(X)dX = -p(x)du(x)\,, \tag{3.26}$$

where $X \equiv g(x - x^{-1})$.

Using eq. (3.25), we can express the expectation value of the "single-trace" operators as

$$\left\langle \mathrm{Tr}\left[\prod_{j=1}^{n} Q_{\ell_j}(M)\right]\right\rangle_J = \oint_{\mathcal{C}} \frac{dX}{2\pi i} \langle R(X)\rangle_J \prod_{j=1}^{n} Q_{\ell_j}(X)\,, \tag{3.27}$$

where $\mathcal{C}$ is a contour which encircles all the eigenvalues X_k's counterclockwise. To proceed, it is convenient to rewrite the above expression in terms of the x, rather than the X, variables. To do so, we need to remember that the x-plane is a double cover of the X-plane and each eigenvalue X_k has two images x_k and $-x_k^{-1}$ in the x-plane. Taking this into account, we obtain the expression

$$\left\langle \mathrm{Tr}\left[\prod_{j=1}^{n} Q_{\ell_j}(M)\right]\right\rangle_J = -\oint_{\mathcal{C}_+\cup\mathcal{C}_-} \frac{du(x)}{4\pi i} \langle p(x)\rangle \prod_{j=1}^{n} Q_{\ell_j}(x)\,, \tag{3.28}$$

where the contours $\mathcal{C}_+$ and $\mathcal{C}_-$ encircle x_k's and $-x_k^{-1}$'s counterclockwise respectively. Note that we used the symmetry of $Q_{\ell_j}(x)$

$$Q_{\ell_j}(x) = Q_{\ell_j}(-x^{-1})\,, \tag{3.29}$$

and the relation eq. (3.26) to get eq. (3.28). The expression eq. (3.28) is valid at finite J. If we take the large J limit, we can approximate $\langle p(x)\rangle$ with its classical value $p_{\mathrm{cl}}(x)$, which was computed[10] in [28]. We then get

$$\left\langle \mathrm{Tr}\left[\prod_{j=1}^{n} Q_{\ell_j}(M)\right]\right\rangle_J \overset{J\to\infty}{=} -\oint_{\mathcal{C}_+\cup\mathcal{C}_-} \frac{du(x)}{4\pi i} p_{\mathrm{cl}}(x) \prod_{j=1}^{n} Q_{\ell_j}(x)\,. \tag{3.30}$$

The classical limit of the quasi-momentum p_{cl} is given in terms of elliptic functions [28], but we do not need its explicit form in this paper. Instead we use its following properties (see also figure 2):

- In the x-plane, $p_{\mathrm{cl}}(x)$ has two (square-root) branch cuts along a unit circle; one along the arc $\mathcal{C}_+ = [e^{-i\theta_0}, e^{i\theta_0}]$ and the other along the arc $\mathcal{C}_- = [-e^{-i\theta_0}, -e^{i\theta_0}]$.

[10] Precisely speaking, the matrix model studied in [28] is different from the one analyzed here. However the large J behavior of the quasi-momentum in the two matrix models was shown to be the same in [12].

JHEP03(2022)020

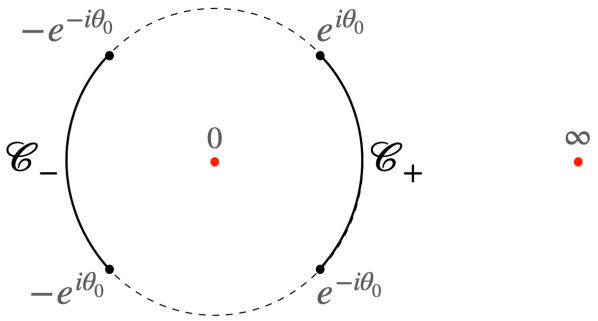

Figure 2. Analytic structure of $p_{\rm cl}(x)$. It has two branch cuts $\mathcal{C}_\pm$, around which the integral $\oint p_{\rm cl}(x)du$ gives $-J$, as well as two poles at $x=0$ and $x=\infty$, around which $\oint p_{\rm cl}(x)dx$ gives J. In addition, $p_{\rm cl}=\pi$ at the *right* branch points, $e^{\pm i\theta}$, and $p_{\rm cl}=-\pi$ at the *left* branch points, $-e^{\pm i\theta}$.

- The parameter θ_0 determining the size of the branch cuts is related to the charge J of the heavy operators by

$$J = 4g\left[\mathbb{K}(\sin^2\theta_0) - \mathbb{E}(\sin^2\theta_0)\right]. \tag{3.31}$$

  Here $\mathbb{K}$ and $\mathbb{E}$ are the complete elliptic integrals of the first and second kind. J is a monotonic function of θ_0 satisfying $J=0$ when $\theta_0=0$ and $J\to\infty$ when $\theta_0\to\pi/2$. As will be explained in section 4, the angle θ_0 also controls the extension of the classical string solution in one of the S^5 directions.

- On the branch cuts, $p_{\rm cl}$ satisfies

$$p_{\rm cl}(x+i0)+p_{\rm cl}(x-i0)=\pm 2\pi \qquad \text{on } \mathcal{C}_\pm\,. \tag{3.32}$$

  In particular, at the branch points, $p_{\rm cl}(x)=\pm\pi$. The integrals around the branch cuts and at $x=0,\infty$ are given by

$$J=\oint_{x=0}p_{\rm cl}(x)du=\oint_{x=\infty}p_{\rm cl}(x)du=-\oint_{\mathcal{C}_+}p_{\rm cl}(x)du=-\oint_{\mathcal{C}_-}p_{\rm cl}(x)du\,. \tag{3.33}$$

- $p_{\rm cl}(x)=-p_{\rm cl}(-x^{-1})$

- The derivative $\partial_J p_{\rm cl}(x)du$ admits a simple expression (see appendix A for the derivation):

$$\partial_J p_{\rm cl}(x)du=\frac{(x+x^{-1})dx}{\sqrt{(x-e^{-i\theta_0})(x-e^{i\theta_0})(x+e^{-i\theta_0})(x+e^{i\theta_0})}}\,. \tag{3.34}$$

Let us also note that, as shown in [28], $p_{\rm cl}(x)$ coincides with the quasi-momentum of the *classical string solution*[11] to be discussed in the next section, which is a holographic dual of the large charge operator on the Wilson loop. This relation is intriguing for several

[11]For the definition of the quasi-momentum in the classical string, see e.g. [51, 52].

JHEP03(2022)020

reasons: first it provides a clear physical interpretation of the spectral curve of our large charge matrix model. (By contrast, an analogous interpretation for the large charge matrix model for $\mathcal{N}=2$ SCFTs has not yet been established at the present time). Second the quasi-momentum of the classical string (and therefore $p_{\rm cl}$ discussed here) is expected to control observables beyond the topological subsector. For instance, in the case of closed string solutions, one can also describe the spectrum of general semi-classical fluctuations using the quasi-momentum as was demonstrated in [36, 37]. We plan to revisit this (in the context of correlation functions) in the upcoming paper [29].

To evaluate eq. (3.30), we deform the contour and bring it around $x=0$ and $x=\infty$. Using the invariance of the integrand under $x\to -x^{-1}$, we then arrive at

$$\left\langle \mathrm{Tr}\left[\prod_{j=1}^{n} Q_{\ell_j}(M)\right]\right\rangle_J \overset{J\to\infty}{=} 2\oint_{x=0}\frac{du(x)}{4\pi i}p_{\rm cl}(x)\prod_{j=1}^{n}Q_{\ell_j}(x)\,, \tag{3.35}$$

where the contour encircles $x=0$ counterclockwise and the factor of 2 comes from the contribution at infinity. Plugging this expression into the large J limit of the formula for the higher-point function eq. (3.22), we obtain

$$\begin{aligned}\frac{\langle\tilde\Phi^J\tilde\Phi^J\prod_{j=1}^{n}\tilde\Phi^{\ell_j}\rangle}{\langle\tilde\Phi^J\tilde\Phi^J\rangle} &\overset{J\to\infty}{=} \oint_{x=0}\frac{du(x)}{2\pi i}\partial_J p_{\rm cl}(x)\prod_{j=1}^{n}Q_{\ell_j}(x)\\ &= \oint_{x=0}\frac{dx(x+x^{-1})}{2\pi i}\frac{\prod_{j=1}^{n}Q_{\ell_j}(x)}{\sqrt{(x-e^{-i\theta_0})(x-e^{i\theta_0})(x+e^{-i\theta_0})(x+e^{i\theta_0})}}\,.\end{aligned} \tag{3.36}$$

The final step is to substitute Q_{ℓ_j} with its strong coupling limit determined in [12],

$$Q_\ell(x)\overset{g\to\infty}{=}(-i)^\ell\left(\frac{g}{2\pi}\right)^{\ell/2}H_\ell\left(i\sqrt{\frac{\pi g}{2}}(x-x^{-1})\right)\,, \tag{3.37}$$

where H_ℓ is the Hermite polynomial. As can be seen from this expression, the leading contribution at large g comes from the highest power in the Hermite polynomial. Therefore, for the purpose of computing the leading answer, we can simplify eq. (3.37) to

$$Q_\ell(x)\overset{g\to\infty}{=}g^\ell(x-x^{-1})^\ell\,. \tag{3.38}$$

Performing the integral in eq. (3.36) analytically, we find that the result is nonzero only when the total length of light operators

$$\ell_{\rm tot}\equiv\sum_{j=1}^{n}\ell_j\,, \tag{3.39}$$

is even, and it is given by

$$\frac{\langle\tilde\Phi^J\tilde\Phi^J\prod_{j=1}^{n}\tilde\Phi^{\ell_j}\rangle}{\langle\tilde\Phi^J\tilde\Phi^J\rangle}\overset{g\to\infty}{=}(-g^2\sin^2\theta_0)^{\ell_{\rm tot}/2}\begin{pmatrix}\ell_{\rm tot}\\ \ell_{\rm tot}/2\end{pmatrix}\,. \tag{3.40}$$

We will later see that this agrees precisely with the result from the classical string.

JHEP03(2022)020

Two-point function. We can also compute the two-point function, $\langle \tilde{\Phi}^J \tilde{\Phi}^J \rangle$, using the matrix model techniques.

For this purpose, we start with the "planar" approximation of the expression eq. (3.11),

$$\langle \tilde{\Phi}^J \tilde{\Phi}^J \rangle = \frac{1}{J+1} \oint d\mu(y) \left\langle \det(Y-M)^2 \right\rangle_J \overset{J\to\infty}{\sim} \frac{1}{J+1} \oint d\mu(y)\, e^{2\langle \mathrm{Tr}\log(Y-M)\rangle_J} \,. \tag{3.41}$$

The exponent can be computed using the matrix model techniques. Namely, we have

$$\langle \mathrm{Tr}\log(Y-M)\rangle_J \overset{J\to\infty}{=} -\oint_{\mathcal{C}_+\cup\mathcal{C}_-} \frac{du(x)}{4\pi i} p_{\mathrm{cl}}(x) \log\left[g(y-x)(1+1/xy)\right] \,. \tag{3.42}$$

To evaluate this integral, we rewrite the logarithmic term as[12]

$$\log\left[g(y-x)(1+1/xy)\right] = \lim_{\Lambda\to\infty} \left[\log(g\Lambda) + \int_\Lambda^y dy' \left(\frac{1}{y'-x} + \frac{1}{y'+1/x} - \frac{1}{y'}\right)\right] \,. \tag{3.43}$$

We then get

$$\begin{aligned} &\langle \mathrm{Tr}\log(Y-M)\rangle_J \overset{J\to\infty}{=} \\ &\lim_{\Lambda\to\infty} \left[J\log(g\Lambda) - \int_\Lambda^y dy' \oint_{\mathcal{C}_+\cup\mathcal{C}_-} \frac{du(x)}{4\pi i} p_{\mathrm{cl}}(x) \left(\frac{1}{y'-x} + \frac{1}{y'+1/x} - \frac{1}{y'}\right)\right] \,. \end{aligned} \tag{3.44}$$

Here we used eq. (3.33) to evaluate $\oint p_{\mathrm{cl}}(x)du$. Next we deform the contour of x and pick up the residues of poles at $x = y', -1/y', 0, \infty$. As a result we obtain

$$\langle \mathrm{Tr}\log(Y-M)\rangle_{L\to\infty} = \lim_{\Lambda\to\infty} \left[J\log(g\Lambda) - \int_\Lambda^{u(y)} p_{\mathrm{cl}}(y')du(y')\right] \,. \tag{3.45}$$

Now, inserting this expression to the original integral eq. (3.41), we find that the integral of y can be evaluated at the saddle point. The saddle point equation receives a contribution from $e^{2\pi g(y+1/y)} = e^{2\pi u(y)}$ in the measure and gives

$$p_{\mathrm{cl}}(y) = \pi \,. \tag{3.46}$$

This condition is satisfied at the right branch points of p_{cl} (i.e., $y = e^{\pm i\theta_0}$). We thus obtain the following expression for the two-point function in the large J limit:

$$\langle \tilde{\Phi}^J \tilde{\Phi}^J \rangle \sim \exp\left(2J\log(g\Lambda) + 2\pi u(e^{i\theta_0}) - 2\int_\Lambda^{u(e^{i\theta_0})} p_{\mathrm{cl}}(x)du\right) \,. \tag{3.47}$$

Here we took $y = e^{i\theta_0}$; the other choice, $e^{-i\theta_0}$, will give the same answer.

Before proceeding, let us make a few comments. The last term in eq. (3.47) can be rewritten as an integral from $x = \Lambda$ on the first sheet (denoted by Λ_+) to $x = -\Lambda$ on the second sheet (denoted by Λ_-):

$$-2\int_\Lambda^{u(e^{i\theta_0})} p_{\mathrm{cl}}(x)du = \int_{\Lambda_-}^{\Lambda_+} p_{\mathrm{cl}}(x)du \,. \tag{3.48}$$

[12] Λ is an artificial cut-off that we introduce solely to write the logarithm as an integral of rational functions with simple poles. This makes the contour deformation analysis easier.

JHEP03(2022)020

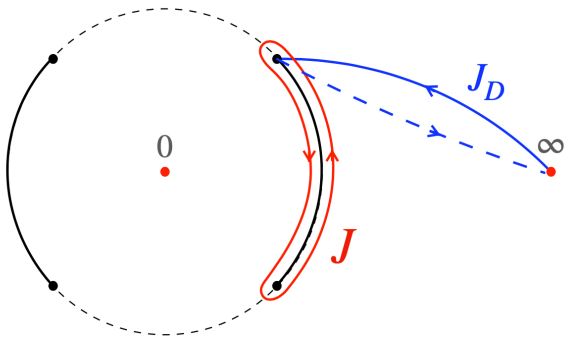

Figure 3. The period integrals on the spectral curve. The charge of the operator, J, is given by an integral of $-p_{\rm cl}du$ around a branch cut. On the other hand, the logarithm of the two-point function, $\log\langle\tilde{\Phi}^J\tilde{\Phi}^J\rangle$, is given (up to terms that come from regularization) by an integral on a "dual" cycle denoted by J_D.

On the other hand, the left hand side of eq. (3.47) is given by a ratio of matrix integrals D_{J+1}/D_J, and it becomes $\exp(\partial_J\mathcal{F}_0)$ in the large J limit, where $\mathcal{F}_0$ is the "genus-0" free energy

$$\log D_J \overset{J\to\infty}{\sim} \mathcal{F}_0\,. \tag{3.49}$$

Note that J is also given by an integral of $p_{\rm cl}(x)du$ albeit on a different contour $\mathcal{C}_\pm$. Therefore eq. (3.47) can be regarded as a relation between period integrals along two "dual" cycles:[13]

$$\begin{aligned}&\partial_J\mathcal{F}_0 = J_D\,,\\ &J = -\oint_{\mathcal{C}_\pm} p_{\rm cl}(x)du\,, \qquad J_D \equiv \int_{\Lambda_-}^{\Lambda_+} p_{\rm cl}(x)du + 2J\log(g\Lambda) + 2\pi u(e^{i\theta_0})\,.\end{aligned} \tag{3.50}$$

See also figure 3. This is an analog of the relations known in conventional large N matrix models and topological strings, which relate the genus 0 free energy with the prepotential of period integrals [53, 54].

Now, to evaluate eq. (3.47), we first differentiate the exponent with respect to J. This gives two contributions: one is proportional to the deformation of the branch point $\partial_J u(y^*)$ while the other comes from the explicit J-dependence in $p_{\rm cl}$ and $J\log(g\Lambda)$. The first contribution is proportional to $\pi - p_{\rm cl}$, which vanishes at the saddle point. Therefore, we only need the second contribution, which gives

$$\begin{aligned}\partial_J\log\langle\tilde{\Phi}^J\tilde{\Phi}^J\rangle &\sim 2\log(g\Lambda) - 2\int_\Lambda^{e^{i\theta_0}} \partial_J p_{\rm cl}(x)du\\ &= 2\log(g\Lambda) - 2\int_\Lambda^{e^{i\theta_0}} dx\frac{x+x^{-1}}{\sqrt{(x-e^{i\theta_0})(x-e^{-i\theta_0})(x+e^{i\theta_0})(x+e^{-i\theta_0})}}\,.\end{aligned} \tag{3.51}$$

This integral can be evaluated analytically, and after sending the cut-off Λ to infinity, we get

$$\partial_J\log\langle\tilde{\Phi}^J\tilde{\Phi}^J\rangle \overset{J\to\infty}{=} \log(-g^2\sin^2\theta_0). \tag{3.52}$$

[13]The extra terms in J_D can be viewed as a regularization which makes the period integral finite.

JHEP03(2022)020

It is useful to pause at this point and switch to the compact notation

$$c \equiv \sin\theta_0. \tag{3.53}$$

Because of eq. (3.31), $c \in [0,1)$ is a monotonic function of J defined implicitly by the relation

$$\frac{J}{4g} = \frac{\mathcal{J}}{4} = \mathbb{K}(c^2) - \mathbb{E}(c^2)\,. \tag{3.54}$$

It satisfies $c = 0$ when $\mathcal{J} = 0$ and $c \to 1$ when $\mathcal{J} \to \infty$. This parametrization of the large charge is convenient in the remainder of the localization analysis in this section, and especially in the dual string analysis in section 4. When we wish to emphasize its J-dependence or let J vary, we will write $c(J)$ instead of c.

Returning to the computation of $\langle \tilde{\Phi}^J \tilde{\Phi}^J \rangle$, it follows from eq. (3.54) that

$$\frac{dJ}{dc^2} = \frac{2g\mathbb{E}(c^2)}{1-c^2}. \tag{3.55}$$

This lets us integrate the c^2-dependent piece of the r.h.s. of eq. (3.52) with respect to J:

$$\begin{aligned}\int_0^J dJ' \log(c^2(J')) &= 2g\int_0^{c^2} dx \frac{\mathbb{E}(x)}{1-x}\log x \\ &= 4g\left[\mathbb{K}(c^2) - \mathbb{E}(c^2)\right]\log(c^2) + 8g\left[\mathbb{E}(c^2) - \mathbb{E}(0)\right] \\ &= \log(c^{2J}) + 8g\left[\mathbb{E}(c^2) - \mathbb{E}(0)\right]\,.\end{aligned} \tag{3.56}$$

Meanwhile, the integral of the l.h.s. of eq. (3.52) yields $\log\langle \tilde{\Phi}^J \tilde{\Phi}^J \rangle - \log\langle 1 \rangle$. Putting everything together, we finally obtain the two-point correlator,

$$\langle\langle \tilde{\Phi}^J \tilde{\Phi}^J \rangle\rangle = \frac{n_J}{(-2)^J} = (-g^2c^2)^J e^{8g\left(\mathbb{E}(c^2)-\mathbb{E}(0)\right)}. \tag{3.57}$$

We will be able to rederive eq. (3.57) from the classical action of the dual string in section 4.

3.3 Large charge correlators from the Bremsstrahlung function

The large charge behavior of the topological two-point correlator can alternatively be determined from the ratio of incrementally shifted two-point functions,

$$R_J \equiv \frac{\langle\langle \tilde{\Phi}^J \tilde{\Phi}^J \rangle\rangle}{\langle\langle \tilde{\Phi}^{J-1} \tilde{\Phi}^{J-1} \rangle\rangle}, \tag{3.58}$$

which can in turn be related to the Bremsstrahlung function, B_J.[14] This lets us take advantage of the leading large charge expression for B_J determined in [28] and the first

[14] The Bremsstrahlung function B_0 was introduced in [18] as a quantity related to the cusp anomalous dimension of the Wilson loop and the radiation emitted by an accelerating quark, and was computed using localization. The generalized Bremsstrahlung function, B_J, was defined and computed using integrability in [28] and computed using localization in [12].

JHEP03(2022)020

subleading correction determined in [55]. We will derive the relation between R_J and B_J using the localization framework developed in [12], which we therefore first briefly summarize.

Firstly, the half-BPS Wilson loop defined in eq. (2.1) can be generalized to a 1/8−BPS Wilson loop [42, 43], $\mathcal{W}_{1/8}$, whose contour $x_\mu(\varphi)$ is any closed curve on the two-sphere $x_1^2+x_2^2+x_3^2=1$ and which couples to the scalars as $\vec{\Phi}\times\vec{x}\cdot d\vec{x}$, where $\vec{x}\equiv(x_1,x_2,x_3)$ and $\vec{\Phi}\equiv(\Phi_3,-\Phi_4,\Phi_6)$.[15] The expectation value of $\mathcal{W}_{1/8}$ is found by replacing $g\to g\frac{A(4\pi-A)}{4\pi^2}$ in eq. (2.2), where A is the area of one of the two regions of the two-sphere demarcated by the contour. The 1/8-BPS loop reduces to the half-BPS loop when $\vec{x}=(\cos\varphi,\sin\varphi,0)$, in which case $A=2\pi$.

Secondly, taking L derivatives of the 1/8-BPS Wilson loop with respect to A inserts L copies of the unit charge topological operator $\tilde{\Phi}\equiv x_1(\varphi)\Phi_3-x_2(\varphi)\Phi_4+x_3(\varphi)\Phi_6+i\Phi_5$,[16] along the loop:

$$\partial_A^L\langle\mathcal{W}_{1/8}\rangle_{\mathcal{N}=4\text{ SYM}}=\langle\mathcal{W}_{1/8}[\underbrace{\tilde{\Phi}\cdots\tilde{\Phi}}_{L}]\rangle_{\mathcal{N}=4\text{ SYM}}. \tag{3.59}$$

For this subsection, we will use $\langle\ldots\rangle_{1/8}\equiv\langle\mathcal{W}_{1/8}[\ldots]\rangle_{\mathcal{N}=4\text{ SYM}}$ to denote the topological defect correlators on the 1/8-BPS loop. These reduce to the topological correlators on the half-BPS Wilson loop when $A=2\pi$. Namely, $\langle\ldots\rangle_{1/8}|_{A=2\pi}=\langle\ldots\rangle$. We also use the notation $\underbrace{\tilde{\Phi}\cdots\tilde{\Phi}}_{L}$ to denote L non-coincident copies of $\tilde{\Phi}$, which is different from the charge L topological operator $\tilde{\Phi}^L$ that can be thought of as the normal-ordered insertion of L coincident copies of $\tilde{\Phi}$.

Thirdly, the higher charge topological operators on the half-BPS Wilson loop can be defined by imposing two properties that are directly parallel to the two properties in eqs. (3.3)–(3.4) defining the Q-functions. Namely,

$$\langle\tilde{\Phi}^J\tilde{\Phi}^M\rangle_{1/8}\propto\delta_{JM}, \tag{3.60}$$

and $\tilde{\Phi}^J$ is a linear combination of the $\underbrace{\tilde{\Phi}\cdots\tilde{\Phi}}_{L}$ operators for $L\leq J$ with a unit leading coefficient:

$$\tilde{\Phi}^J=\underbrace{\tilde{\Phi}\cdots\tilde{\Phi}}_{J}+\ldots. \tag{3.61}$$

In this way the higher charge topological operators define an orthogonal basis that can be constructed from non-coincident insertions of the unit topological operators using the Gram-Schmidt procedure.

[15] We pick this combination of scalar fields to couple to the 1/8-BPS Wilson loop in order to match our conventions for the half-BPS Wilson loop and topological operators in section 2.

[16] More generally, we may equivalently define the topological operator to be $\vec{x}(\varphi)\cdot\vec{\Phi}+i\hat{n}\cdot\vec{\Phi}^\perp$, where $\vec{\Phi}^\perp\equiv(\Phi_1,\Phi_2,\Phi_5)$ and $\hat{n}$ is any unit 3-vector. We use the freedom to pick $\hat{n}=(0,0,1)$ so that this topological operator reduces to the topological operator defined in eq. (2.10) when the 1/8-BPS Wilson loop reduces to the half-BPS Wilson loop.

JHEP03(2022)020

Finally, the topological correlators are closed under the OPE. As a special case, the OPE between a charge J insertion and a unit charge is simply

$$\tilde{\Phi}^J\,\tilde{\Phi} = \tilde{\Phi}^{J+1} + \frac{\langle \tilde{\Phi}^J\,\tilde{\Phi}^J\rangle_{1/8}}{\langle \tilde{\Phi}^{J-1}\,\tilde{\Phi}^{J-1}\rangle_{1/8}}\tilde{\Phi}^{J-1}\,. \tag{3.62}$$

The prefactors on the r.h.s. of eq. (3.62) can be determined by taking the expectation value after multiplying both sides above by $\tilde{\Phi}^{J+1}$ or $\tilde{\Phi}^{J-1}$, and also noting that

$$\langle \tilde{\Phi}\,\tilde{\Phi}^J\,\tilde{\Phi}^{J+1}\rangle_{1/8} = \langle \tilde{\Phi}^{J+1}\,\tilde{\Phi}^{J+1}\rangle_{1/8}\,. \tag{3.63}$$

This is a special case of the statement that the extremal topological correlators, for which the largest charge is equal to the sum of all the smaller charges, reduce to two-point functions. Namely,

$$\langle \tilde{\Phi}^{J_1}\tilde{\Phi}^{J_2}\ldots\tilde{\Phi}^{J_n}\rangle_{1/8} = \langle \tilde{\Phi}^{J_1}\tilde{\Phi}^{J_1}\rangle_{1/8}\,, \qquad \text{if } J_1 = J_2 + \ldots + J_n, \tag{3.64}$$

as was shown in [12].

We have now laid all of the groundwork needed to relate the topological two-point function to the Bremsstrahlung function. We begin with the expression derived in [12] (see also [18]) for the Bremsstrahlung function as the second area derivative of the two-point function:

$$B_J = -\partial_A^2 \log \langle \tilde{\Phi}^J\tilde{\Phi}^J\rangle_{1/8}\Big|_{A=2\pi}\,. \tag{3.65}$$

Each area derivative in eq. (3.65) can either act on the Wilson loop to insert a factor of $\tilde{\Phi}$ or on one of the topological operators. In particular, when we expand

$$\tilde{\Phi}^J = \underbrace{\tilde{\Phi}\cdots\tilde{\Phi}}_{J} + c_J(A)\,\underbrace{\tilde{\Phi}\cdots\tilde{\Phi}}_{J-1} + \ldots\,, \tag{3.66}$$

then all the coefficients other than the leading one depend on the area. We have explicitly labelled the next-to-leading coefficient, $c_J(A)$, since it plays an important role in what follows. Eq. (3.65) therefore evaluates to

$$-B_J = \frac{\langle \tilde{\Phi}^J\tilde{\Phi}^J\tilde{\Phi}\tilde{\Phi}\rangle}{\langle \tilde{\Phi}^J\tilde{\Phi}^J\rangle} + 2\frac{dc_J}{dA}\Big|_{A=2\pi}\,. \tag{3.67}$$

Various other terms on the r.h.s. drop out due to the orthogonality in eq. (3.60). The next step is to deduce a more transparent form for $\frac{dc_J}{dA}$. Taking one area derivative of $\langle \tilde{\Phi}^J\tilde{\Phi}^{J-1}\rangle = 0$ yields

$$\frac{dc_J}{dA}\Big|_{A=2\pi} = -\frac{\langle \tilde{\Phi}^J\tilde{\Phi}^{J-1}\tilde{\Phi}\rangle}{\langle \tilde{\Phi}^{J-1}\tilde{\Phi}^{J-1}\rangle} = -R_J. \tag{3.68}$$

To get to the second equality, we used eq. (3.63) and recalled the definition of R_J in eq. (3.58).

JHEP03(2022)020

Finally, applying the OPE in eq. (3.62) to both copies of $\tilde{\Phi}^J\tilde{\Phi}$ in the four point correlator on the r.h.s. of eq. (3.67), we can write it in terms of R_J as well:

$$\frac{\langle\tilde{\Phi}^J\tilde{\Phi}^J\tilde{\Phi}\tilde{\Phi}\rangle}{\langle\tilde{\Phi}^J\tilde{\Phi}^J\rangle} = R_{J+1} + R_J. \tag{3.69}$$

Therefore, eqs. (3.67), (3.68) and (3.69) yield

$$-B_J = R_{J+1} - R_J, \tag{3.70}$$

which is the desired relation for R_J in terms of B_J. It holds for any g and J.

We are in particular interested in eq. (3.70) in the large charge regime. If we expand R_J and B_J in $1/g$,

$$R_J \equiv g^2 r_2\left(J/g\right) + g r_1(J/g) + \ldots, \tag{3.71}$$
$$B_J \equiv g b_1(J/g) + b_0(J/g) + \ldots, \tag{3.72}$$

then we can use eq. (3.70) to relate r_2 and r_1 to b_1 and b_0. The latter two were determined in [28, 55]:

$$b_1(J/g) = \frac{1-c^2}{2\mathbb{E}(c^2)}, \qquad b_0(J/g) = \frac{1}{2}b_1'(J/g). \tag{3.73}$$

Here, we have written b_1 in terms of the parameter c^2 introduced in eq. (3.54), and have found that b_0 simplifies when written in terms of b_1.[17] Substituting eqs. (3.71) and (3.72) into eq. (3.70) and matching the two sides order by order yields the following pair of differential equations:

$$r_2'(x) = -b_1(x), \qquad \frac{1}{2}r_2''(x) + r_1'(x) = -b_0(x). \tag{3.74}$$

Eqs. (3.73) and (3.74) together imply $r_1'(x) = 0$. Furthermore, writing $r_2'(J/g) = g\frac{dr_2}{dc^2}\frac{dc^2}{dJ}$ and noting from eq. (3.55) that $b_1(J/g) = g\frac{dc^2}{dJ}$, we find $\frac{dr_2}{dc^2} = -g^2$. Finally, imposing the initial conditions $r_2(0) = r_1(0) = 0$,[18] we arrive at the following particularly simple form for R_J:

$$R_J = -g^2c^2 + O(g^0). \tag{3.75}$$

[17] To get this result, we set $r = 1$ and $\sin^2\psi = c^2$ in eqs. (5.11) and (5.12) of [55].

[18] These initial conditions can be justified as follows. As we'll discuss in section 4.4, the small $\mathcal{J}$ expansion of the large charge correlators matches the large J expansion of the strongly coupled finite charge correlators. Thus, we can partly determine the behavior of R_J as $\mathcal{J} \to 0$ using the expression for the finite charge correlator determined in [12], which is given in eq. (3.81). From

$$R_J = -\frac{n_J}{2n_{J-1}} = -\frac{gJ}{\pi}\left(1 - \frac{3J}{8\pi g} + O(1/g^2)\right) = g^2\left(-\frac{\mathcal{J}}{\pi} + \frac{3\mathcal{J}^2}{8\pi^2 g} + O(\mathcal{J}^3)\right) + gO(\mathcal{J}^2) + O(g^0),$$

we explicitly see that $r_2 \to 0$ and $r_1 \to 0$ as $\mathcal{J} \to 0$.

JHEP03(2022)020

Eq. (3.75) lets us determine the large charge limit of the two-point correlator. Keeping only the leading order term in R_J, we find

$$\langle\langle \tilde{\Phi}^J \tilde{\Phi}^J \rangle\rangle = \prod_{j=1}^{J} R(j) = (-g^2)^J \exp\left(\sum_{j=1}^{J} \log c^2(j)\right). \tag{3.76}$$

To leading order, we may approximate the sum by the integral computed in eq. (3.56). This reproduces the result in the previous subsection, eq. (3.57).

Returning to eq. (3.69), eq. (3.75) also lets us determine the four-point correlator:

$$\frac{\langle \tilde{\Phi}^J \tilde{\Phi}^J \tilde{\Phi} \tilde{\Phi} \rangle}{\langle \tilde{\Phi}^J \tilde{\Phi}^J \rangle} = 2R_J - B_J = -2g^2c^2 - \frac{g}{2}\frac{1-c^2}{\mathbb{E}(c^2)} + O(g^0). \tag{3.77}$$

We will see in section 4 that, in the dual string calculation, $2R_J$ is the classical contribution to the four point function. The other term, $-B_J$, corresponds to the contribution from semiclassical fluctuations, which we will discuss in [29].

Finally, eq. (3.75) also lets us determine the normalized extremal OPE coefficient,

$$\frac{c^2_{J+\ell,J,\ell}}{n_{J+\ell} n_J n_\ell} \equiv \frac{\langle\langle \tilde{\Phi}^{J+\ell} \tilde{\Phi}^J \Phi^\ell \rangle\rangle^2}{\langle\langle \Phi^{J+\ell} \Phi^{J+\ell} \rangle\rangle \langle\langle \Phi^J \Phi^J \rangle\rangle \langle\langle \Phi^\ell \Phi^\ell \rangle\rangle}, \tag{3.78}$$

to next-to-leading order. We first note from eq. (3.55) how c changes when J changes by a finite amount:

$$c^2(J+j) = c^2 + \frac{j}{2g}\frac{1-c^2}{\mathbb{E}(c^2)} + O(j^2/J^2). \tag{3.79}$$

Therefore,

$$\frac{\langle \tilde{\Phi}^{J+\ell} \tilde{\Phi}^{J+\ell} \rangle}{\langle \tilde{\Phi}^J \tilde{\Phi}^J \rangle} = \prod_{j=1}^{\ell} R_{J+j} = (-g^2c^2)^\ell \left(1 + \frac{\ell(\ell+1)}{4g}\frac{1-c^2}{c^2\mathbb{E}(c^2)} + O(1/g^2)\right). \tag{3.80}$$

Noting the strong coupling expansion of n_ℓ for finite ℓ [12],

$$n_\ell(g) = \left(\frac{2g}{\pi}\right)^\ell \ell! \left(1 - \frac{3}{16\pi g}\ell(\ell+1) + O(1/g^2)\right), \tag{3.81}$$

the normalized extremal OPE coefficient becomes

$$\frac{c^2_{J+\ell,J,\ell}}{n_{J+\ell} n_J n_\ell} = \frac{(g\pi c^2)^\ell}{\ell!}\left(1 + \frac{\ell(\ell+1)}{4g}\left[\frac{3}{4\pi} + \frac{1-c^2}{c^2\mathbb{E}(c^2)}\right] + O(1/g^2)\right). \tag{3.82}$$

4 Large charge correlators from the classical string

Now we turn to the analysis of the large charge correlators using the classical string solution in $AdS_5 \times S^5$ that is holographically dual to the Wilson operator with Z^J and $\bar{Z}^J$ inserted.

The classical string was discussed previously in a few closely related contexts. The string with $\mathcal{J} \to \infty$ was first identified in [9], and its spectrum of fluctuations in the BMN

JHEP03(2022)020

limit was matched to the anomalous dimensions, computed in weakly coupled gauge theory, of "words" inserted on the Wilson loop that are composed of many copies of Z interspersed with a few copies of an orthogonal scalar. Then [30] used the same classical string to explore the $\mathcal{J} \to \infty$ limit of the two-point function in eq. (2.16). Finally, the string with general $\mathcal{J}$ is a special case of a more general string solution identified in appendix E of [28], which was used to determine the classical limit of the cusp anomalous dimension of the Wilson line with cusps simultaneously in both the ambient and internal contours at the locations of the Z^J and $\bar{Z}^J$ insertions. (In our analysis the Wilson loop has insertions but no cusps.)

We will first review the general $\mathcal{J}$ string solution and, as an additional check building on the previous works, we show in appendix B that the supersymmetries of the dual string match those of the Wilson loop with insertions by extending the discussion in section 4.2 of [9] to the case with general $\mathcal{J}$. The main new results of our analysis are the evaluation of the classical action of the string solution (including the identification of the relevant boundary terms), which gives the holographic prediction for the two-point function of the large charge insertions, and the calculation of higher-point correlators with two heavy charges using the classical string.

4.1 Identifying the dual string solution

In this section, generalizing section 4.1 in [9], we identify the classical string dual to the Wilson operator with Z^J and $\bar{Z}^J$ inserted and $\mathcal{J}$ finite. We begin by writing the metric in $\text{AdS}_5 \times S^5$ using global coordinates on AdS_5 and embedding coordinates on S^5:

$$ds^2 = ds^2_{\text{AdS}_5} + ds^2_{S^5}, \tag{4.1}$$

where

$$\begin{aligned} ds^2_{\text{AdS}_5} &= d\rho^2 - \cosh^2\rho dt^2 + \sinh^2\rho \left(d\psi_1^2 + \sin^2\psi_1 \left(d\psi_2^2 + \sin^2\psi_2 d\psi^2\right)\right) \\ ds^2_{S^5} &= d\Theta_I d\Theta_I. \end{aligned} \tag{4.2}$$

Here, $\rho \in [0, \infty)$ is the bulk coordinate of AdS_5 such that $\rho = 0$ is the middle of AdS_5 and $\rho \to \infty$ is the conformal boundary, $\mathbb{R} \times S^3$; t is the time coordinate along $\mathbb{R}$; and $\psi_1, \psi_2 \in [0, \pi]$ and $\psi \in [0, 2\pi)$ are spherical coordinates on S^3. Furthermore, the coordinates Θ_I, $I = 1, \ldots 6$, satisfy $\Theta_I \Theta_I = 1$ and embed S^5 in $\mathbb{R}^6$.

We let the contour of the half-BPS Wilson operator on the boundary consist of the two antiparallel, antipodal lines that lie at $\rho \to \infty, \psi_1 = \psi_2 = \frac{\pi}{2}$ and $\psi = 0, \pi$, such that the line at $\psi = 0$ runs in the positive t direction and the line at $\psi = \pi$ runs in the negative t direction. Furthermore, we put Z^J in the infinite past, $t \to -\infty$, and $\bar{Z}^J$ in the infinite future, $t \to \infty$. Given this symmetric choice of the Wilson contours in global coordinates, we may restrict our attention to the AdS_3 subspace of AdS_5 with $\psi_1 = \psi_2 = \frac{\pi}{2}$. We could also fix $\psi = 0, \pi$ and restrict to an AdS_2 subspace but it is convenient to keep track of ψ for when we ultimately change to Poincaré coordinates and map this configuration to the circular Wilson loop with two insertions at $\varphi = \pm\varphi_L$, as in eq. (2.16).

The coordinate Θ_I is dual to Φ_I. Since the Wilson loop couples only to Φ_6 and the insertions Z^J and $\bar{Z}^J$ are composed of only Φ_4 and Φ_5, it follows that the dual string also

JHEP03(2022)020

lies in the S^2 subspace of S^5 defined by $\Theta_4^2+\Theta_5^2+\Theta_6^2=1$, $\Theta_1=\Theta_2=\Theta_3=0$. We introduce the coordinates $\theta\in[0,\pi]$ and $\phi\in[0,2\pi)$ to parametrize this two-sphere such that θ is the polar angle from the north pole, $\Theta_6=1$, and ϕ is the azimuthal angle that rotates parallel to the Θ_4-Θ_5 plane:

$$\Theta_4=\sin\theta\cos\phi, \qquad \Theta_5=\sin\theta\sin\phi, \qquad \Theta_6=\cos\theta. \tag{4.3}$$

Therefore, restricting to the $\mathrm{AdS}_3\times S^2$ subspace that contains the dual string, we may write the relevant parts of the metric as

$$ds^2=ds^2_{\mathrm{AdS}_3}+ds^2_{S^2}, \tag{4.4}$$

$$ds^2_{\mathrm{AdS}_3}=d\rho^2-\cosh^2\rho dt^2+\sinh^2\rho d\psi^2, \qquad ds^2_{S^2}=d\theta^2+\sin^2\theta d\phi^2. \tag{4.5}$$

It is convenient to extend ρ to negative values and identify $(-\rho,t,\psi)=(\rho,t,\psi+\pi)$.

The string moving in the background in eq. (4.4) is governed by the Nambu-Goto action (recall that we use the notation $g\equiv\frac{\sqrt{\lambda}}{4\pi}$),

$$S_{\mathrm{NG}}[\Psi]=-2g\int d^2\sigma\sqrt{-h}, \tag{4.6}$$

where Ψ is shorthand for the all the coordinates of the string, $2g$ is the string tension, σ^α, $\alpha=0,1$, are the worldsheet coordinates, and h denotes the determinant of $h_{\alpha\beta}$, the metric induced on the worldsheet. Following [9], we identify the classical string dual to the Wilson operator with Z^J and $\bar{Z}^J$ in the large charge limit as the solution extremizing eq. (4.6) with the following properties:

1. The string is incident on the antiparallel lines at $\psi=0,\pi$ on the boundary of AdS_3 and is at $\theta=0$, the north pole of S^2, when it reaches the boundary.

2. As the string moves away from the antiparallel lines on the boundary, it simultaneously moves away from the north pole in S^2 and reaches a maximum angle, $\theta_0\in[0,\pi/2)$, when it reaches the middle of AdS_3.

3. The string rotates in S^2 in the ϕ direction with angular momentum J.

A family of string solutions satisfying the equations of motion and having the first two properties is given by:

$$\begin{aligned} \rho&=\sigma^1, \qquad & t&=\sigma^0, \qquad & \psi&=0,\\ \sin\theta&=\frac{c}{\cosh\sigma^1}, \qquad & \phi&=\phi_0+\sigma^0. \end{aligned} \tag{4.7}$$

Here, the worldsheet coordinates, $\sigma^1\equiv\rho$ and $\sigma^0\equiv t$, span $\mathbb{R}$, the parameter $c\in[0,1)$ is related to the maximum value of θ by

$$c=\sin\theta_0\,, \tag{4.8}$$

and $\phi_0\in[0,2\pi)$ is a modulus whose significance will become clear in the next section. The string is depicted in figure 4. While we have presented the string solution using the

JHEP03(2022)020

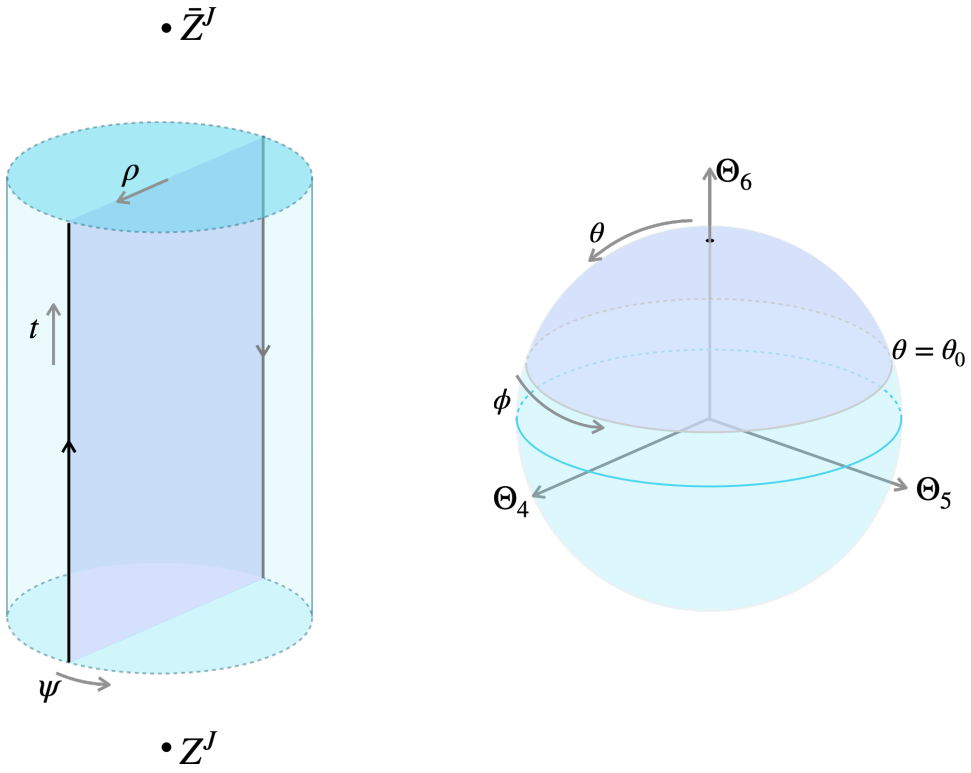

a. Classical string solution in AdS_5 **b.** Classical string solution in S^5

Figure 4. The classical string solution in $AdS_5 \times S^5$ dual to the Wilson loop operator with Z^J and $\bar{Z}^J$. **a.** In global AdS_5 coordinates, the string forms a strip stretching between the antipodal, antiparallel lines forming the contour of the Wilson operator. The insertions, Z^J and $\bar{Z}^J$, are located at the infinite past and future, respectively. **b.** In S^5, the string wraps part of the upper half of the two-sphere $\Theta_4^2 + \Theta_5^2 + \Theta_6^2 = 1$. When the string is at the boundary of AdS, $\rho \to \pm\infty$, it is at the north pole of the sphere, $\theta = 0$. When the string is in the center of AdS, $\rho = 0$, it is at the maximum polar angle on the sphere, $\theta = \theta_0$. Furthermore, translations in t in AdS are accompanied by rotations in ϕ on the sphere.

Nambu-Goto description, one may also use the conformal gauge and the Polyakov action, as in [9, 28]. The solution in the conformal gauge is related to eq. (4.7) by a change of variable of the σ^2 coordinate (involving elliptic functions) with $\sigma^0 = t$ unchanged. We find it more convenient to work with the Nambu-Goto action and the solution eq. (4.7).

Finally, to complete the identification of the classical string dual to the Wilson loop operator with insertions, we require that it have the correct angular momentum in accordance with the third property above. This fixes the value of the parameter c in terms of the charge J. Noting the angular momentum density $\Pi_\phi \equiv -2g\frac{\partial\sqrt{-h}}{\partial(\partial_0\phi)} = -2g\sin^2\theta\sqrt{-h}h^{0\alpha}\partial_\alpha\phi$, and setting the anguluar momentum of the string equal to J, we find

$$J = \int_{-\infty}^{\infty} d\rho \Pi_\phi = 2g\int_{-\infty}^{\infty} d\rho \frac{c^2\,\mathrm{sech}^2\,\rho}{\sqrt{\cosh^2\rho - c^2}} = 4g(\mathbb{K}(c^2) - \mathbb{E}(c^2)), \tag{4.9}$$

which matches eq. (3.54) derived from the matrix model side. This tells us that the

JHEP03(2022)020

maximum polar angle of the classical string is the same as the angle parametrizing the branch cuts of $p_{\rm cl}$ (see figure 2), which justifies our use of the same symbol, θ_0, for both. Therefore, we may also identify the parameter c in the string solution in eq. (4.7) with the parameter introduced in eq. (3.53). In fact, as shown in [36], the classical quasi-momentum of the matrix model coincides with that obtained from the string solution.

To connect our discussion above with previous work, we note that the string solution found in [9] is given by eq. (4.7) when $\mathcal{J} \to \infty$ or $c = 1$. The classical string we consider is a simple generalization of the $c = 1$ string that preserves the same supersymmetries, as we check explicitly in appendix B. It is in turn a special case of the string considered in [28] when the Wilson loop on the boundary does not have cusps in either the ambient contour or the internal contour at the locations of the two insertions.[19]

To close this section, we transform the solution in eq. (4.7) into a form more suitable for computing correlations functions on the Wilson loop. We begin by continuing from Lorentzian to Euclidean signature, letting $t = -i\tau$ where $\tau \in \mathbb{R}$ is Euclidean time. Then $\phi = \phi_0 - i\tau$ in (4.7), and the Euclidean action is $S_{\rm NG} = 2g \int d^2\sigma \sqrt{h}$. The Euclidean worldsheet coordinates will be denoted by $\sigma^1 = \rho$ and $\sigma^2 \equiv i\sigma^0 = \tau$. Secondly, as an intermediate step, we map the solid cylinder in global coordinates to the half-volume in Poincaré coordinates using the transformation

$$z' = \frac{1}{\cosh\rho\cosh\tau + \sinh\rho\cos\psi}, \qquad x_1' = z'\sinh\rho\sin\psi, \qquad x_2' = z'\sinh\tau\cosh\rho. \tag{4.10}$$

This maps the Wilson contour to the line $x_1' = 0$ on the boundary $z' = 0$ and sends Z^J to $x_2' = -1$ and $\bar{Z}^J$ to $x_2' = 1$. It maps the dual string to the half-plane $x_1' = 0$. See figure 5a.

Next, we shift the string in the x_1' direction by $a \equiv \cot\left(\frac{\varphi_L}{2}\right)$ and then invert, rescale and recenter to get the transformation

$$z = \frac{2az'}{z'^2 + (x_1'+a)^2 + x_2'^2}, \qquad x_1 = \frac{a^2 - x_1'^2 - x_2'^2 - z'^2}{z'^2 + (x_1'+a)^2 + x_2'^2}, \qquad x_2 = \frac{2ax_2'}{z'^2 + (x_1'+a)^2 + x_2'^2}. \tag{4.11}$$

This maps the Wilson contour to the circle $(x_1, x_2) = (\cos\varphi, \sin\varphi)$ on the boundary $z = 0$ and sends Z^J to $\varphi = -\varphi_L$ and $\bar{Z}^J$ to $\varphi = \varphi_L$. It maps the dual string to the hemisphere $x_1^2 + x_2^2 + z^2 = 1$. See figure 5b.

Therefore, the composition of eqs. (4.10) and (4.11) produces the classical string in $\mathrm{EAdS}_3 \times S^2 \subset \mathrm{EAdS}_5 \times S^5$ that we can use to study the large charge correlator in eq. (2.16). The solution in these coordinates takes the explicit form

$$\begin{gathered} z = \frac{\sin\varphi_L}{\Delta}, \quad x_1 = \frac{\cos\varphi_L\cosh\tau\cosh\rho + \sinh\rho}{\Delta}, \quad x_2 = \frac{\sin\varphi_L\sinh\tau\cosh\rho}{\Delta}, \\ \sin\theta = \frac{c}{\cosh\rho}, \quad \phi = \phi_0 - i\tau\,, \quad \Delta = \cosh\tau\cosh\rho + \cos\varphi_L\sinh\rho. \end{gathered} \tag{4.12}$$

When $c = 1$, this solution is essentially equivalent to the one in [30].

The string in eq. (4.12) is incident on Z^J at $\varphi = -\varphi_L$ as $\tau \to -\infty$, on $\bar{Z}^J$ at $\varphi = \varphi_L$ as $\tau \to \infty$, and on the unit circle as $\rho \to \pm\infty$. To approach the specific point φ on the

[19] Specifically, to match the string solution defined in eq. (4.7) to the one in [28], the parameters ℓ_θ, ℓ_ϕ, κ and γ in appendix E.1 of [28] should be set to $\ell_\theta = \ell_\phi = 0$ and $\kappa = \gamma = \frac{1}{c}$.

JHEP03(2022)020

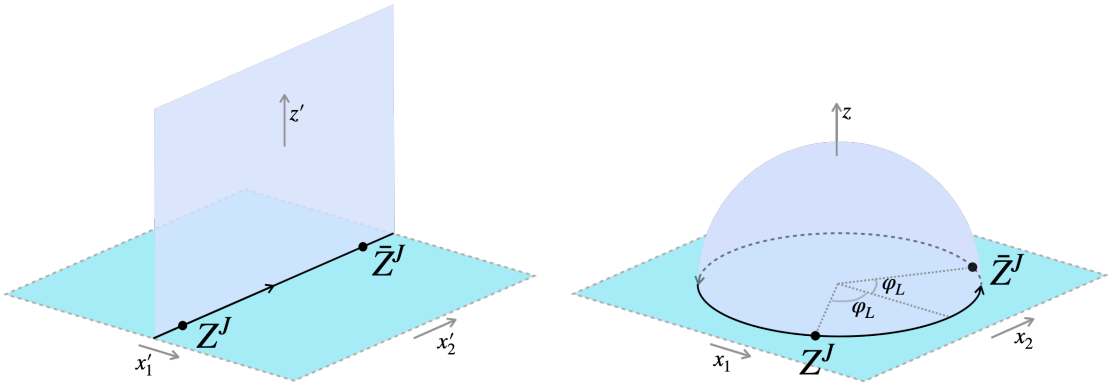

a. Half-plane **b.** Hemisphere

Figure 5. The classical string solution in AdS global coordinates in figure 4 can be mapped to: **a.** a half-plane in Poincaré coordinates using eq. (4.10), in which case the string is dual to the Wilson line $x_1' = 0$ with Z^J and $\bar{Z}^J$ at $x_2' = \mp 1$; or to **b.** the hemisphere in Poincaré coordinates using eq. (4.11), in which case the classical string is dual to the Wilson loop $x_1^2 + x_2^2 = 1$ with Z^J and $\bar{Z}^J$ at $\varphi = \mp\varphi_L$.

circle from the worldsheet, we fix τ and send $\rho \to \eta\infty$, where $\eta = +1$ for $\varphi \in [-\varphi_L, \varphi_L]$ and $\eta = -1$ otherwise and τ is determined by the pair of implicit equations

$$\frac{\cosh\tau \pm \sinh\tau}{\cosh\tau + \eta\cos\varphi_L} = 2\sin^2\left(\frac{\varphi \pm \varphi_L}{2}\right) / \sin^2\varphi_L. \tag{4.13}$$

This follows from eq. (4.12) and we have expressed it in terms of the chordal distances from φ to the insertions.

A note about notation: going forward, we will continue to write $d^2\sigma \equiv d\rho d\tau$ for the measure on the worldsheet and use α and β as free or summed worldsheet indices, but we will label particular components of worldsheet tensors using ρ, τ instead of $1, 2$.

4.2 Two-point function

The two-point correlator in eq. (2.16) can be computed using a semiclassical evaluation of the string path integral of the appropriate vertex operators weighted by the action:

$$\langle\langle Z^J(-\varphi_L)\bar{Z}^J(\varphi_L)\rangle\rangle = \frac{\int D\Psi e^{-S[\Psi]}\ v^J(-\varphi_L;\Psi)\bar{v}^J(\varphi_L;\Psi)}{\int D\Psi\ e^{-S[\Psi]}}. \tag{4.14}$$

Here $\int D\Psi$ is the path integral over all the fields in the superstring sigma model, which are collectively denoted by Ψ. Furthermore, v and $\bar{v}$ are the vertex operators dual to Z and $\bar{Z}$, which are determined by sending the insertions of $\Theta_4 \pm i\Theta_5 = \sin\theta e^{\pm i\phi}$ to the boundary of the world sheet:

$$v(\varphi;\Psi) \equiv 2g \lim_{\rho\to\eta\infty} \frac{\sin\theta e^{i\phi}}{z}, \qquad \bar{v}(\varphi;\Psi) \equiv 2g \lim_{\rho\to\eta\infty} \frac{\sin\theta e^{-i\phi}}{z}. \tag{4.15}$$

The limits are taken in accordance with eq. (4.13). We have defined the vertex operators with the usual factor of $1/z$ (recall that the unit charge chiral primaries have unit conformal

JHEP03(2022)020

dimension) that appears in the AdS/CFT dictionary when extrapolating bulk points to the boundary. The vertex operators also include the natural string tension factor $2g = \frac{\sqrt{\lambda}}{2\pi}$. And, finally, $S[\Psi]$ in eq. (4.14) is the complete action of the string, which is the sum of the Nambu-Goto action and a boundary action:

$$S[\Psi] \equiv S_{\rm NG}[\Psi] + S_{\rm bdy}[\Psi]. \tag{4.16}$$

Identifying $S_{\rm bdy}[\Psi]$ is the focus of the next section.

In the large charge regime, the path integral in eq. (4.14) is dominated by the classical string solution given in eq. (4.12), which we shall schematically denote $\Psi_{\rm cl}(c, \phi_0, \varphi_L)$ (or $\Psi_{\rm cl}(c)$ when we only want to emphasize the c-dependence). The action and the vertex operators in eq. (4.14) can therefore be evaluated on this solution. Let us adopt the shorthand

$$S_{\rm cl}(c) \equiv S[\Psi_{\rm cl}(c, \phi_0, \varphi_L)] \tag{4.17}$$

for the classical action of the string, and

$$v_{\rm cl}(\varphi) \equiv v(\varphi; \Psi_{\rm cl}(c, \phi_0, \varphi_L)), \qquad \bar{v}_{\rm cl}(\varphi) \equiv \bar{v}(\varphi; \Psi_{\rm cl}(c, \phi_0, \varphi_L)) \tag{4.18}$$

for the vertex operators evaluated on the classical string solution. The action $S_{\rm cl}(c)$ does not depend on ϕ_0 or φ_L, since changing ϕ_0 is implemented by an isometry on S^2 and changing φ_L is implemented by an isometry on EAdS_3. By contrast, the vertex operators, $v_{\rm cl}$ and $\bar{v}_{\rm cl}$, do depend on c, ϕ_0 and φ_L as well as on φ, but we drop the explicit dependence for ease of notation. The two-point function in the large charge limit therefore becomes

$$\langle\langle Z^J(-\varphi_L)\bar{Z}^J(\varphi_L)\rangle\rangle = \frac{1}{2\pi}\int_0^{2\pi} d\phi_0\; v_{\rm cl}^J(-\varphi_L)\bar{v}_{\rm cl}^J(\varphi_L)e^{-S_{\rm cl}(c)+S_{\rm cl}(0)}. \tag{4.19}$$

The term $S_{\rm cl}(0)$ in the exponent comes from the denominator in eq. (4.14). To understand and apply eq. (4.19), we need to understand the origin of the integral over ϕ_0, determine the classical vertex operators, $v_{\rm cl}$ and $\bar{v}_{\rm cl}$, and evaluate the classical action $S_{\rm cl}(c) - S_{\rm cl}(0)$.

We begin with the integral over ϕ_0. Recall that moduli of classical solutions play an important role in relating the observables in semiclassical eigenstates of a quantum mechanical system to the observables along trajectories of the corresponding classical system. The quantum mechanical counterpart of a family of classical trajectories labelled by a modulus is a family of coherent states rather than eigenstates. Since a particular eigenstate can be realized by a suitable linear combination of the coherent states, one should suitably average the expectation values of the classical trajectories over the moduli to reproduce the quantum expectation value. See sections 2–3 of [33] and also [32] for discussions. In our case, the semiclassical string with a given ϕ_0 is dual to a coherent state of average charge J, and integrating over ϕ_0 in eq. (4.19) ensures that the resulting expectation value on the l.h.s. is for an eigenstate of charge J.

Next, we note the explicit form of the vertex operators on the classical string:

$$\begin{aligned} v_{\rm cl}(\varphi) &= 2g\lim_{\rho\to\eta\infty}\frac{\Delta}{\sin\varphi_L}\frac{c}{\cosh\rho}e^{i\phi_0+\tau} = 2gce^{i\phi_0}\frac{d}{d(\varphi,\varphi_L)^2} \\ \bar{v}_{\rm cl}(\varphi) &= 2g\lim_{\rho\to\eta\infty}\frac{\Delta}{\sin\varphi_L}\frac{c}{\cosh\rho}e^{-i\phi_0-\tau} = 2gce^{-i\phi_0}\frac{d}{d(\varphi,-\varphi_L)^2}\,, \end{aligned} \tag{4.20}$$

JHEP03(2022)020

where Δ was defined in eq. (4.12). Above we used eq. (4.13) to evaluate the limit in terms of φ instead of τ and wrote the result in terms of the chordal distances introduced in eq. (2.5). Thus, the contribution of the large charge vertex operators to the r.h.s. of eq. (4.19) is[20]

$$v_{\rm cl}^J(-\varphi_L)\bar{v}_{\rm cl}^J(\varphi_L) = \frac{(2gc)^{2J}}{d^{2J}}. \tag{4.21}$$

This has the correct position dependence for a conformal two-point correlator, as in eq. (2.16). Furthermore, the factors of $e^{i\phi_0}$ and $e^{-i\phi_0}$ from the two vertex operators evidently cancel and the integral over ϕ_0 in eq. (4.19) simply yields 1. Stated differently, given the explicit forms of the vertex operators in eq. (4.20), the integral over ϕ_0 ensures that the r.h.s. of eq. (4.19) is nonzero only if equal numbers of $v_{\rm cl}$ and $\bar{v}_{\rm cl}$ are inserted on the boundary of the worldsheet. This mirrors the requirement from R-symmetry that the l.h.s. is nonzero only if equal numbers of Z and $\bar{Z}$ are inserted along the Wilson loop. The role of the integration over ϕ_0 will be slightly less trivial when we consider higher-point functions below.

The last step in evaluating eq. (4.19) is to determine the value of the action on the classical string solution, $S_{\rm cl}(c)$. For simplicity we compute the action for the case of antipodal insertions, which is equal to the action for the case with general insertions. Setting $\varphi_L = \pi/2$, the form of the string in EAdS$_3$ simplifies to

$$z = \frac{1}{\cosh\tau\cosh\rho}, \qquad x_1 = \frac{\tanh\rho}{\cosh\tau}, \qquad x_2 = \tanh\tau. \tag{4.22}$$

We also note the explicit form of the metric induced on the worldsheet,

$$h_{\rho\rho} = \frac{\cosh^4\rho - c^2}{\cosh^4\rho - c^2\cosh^2\rho}, \qquad h_{\tau\tau} = \cosh^2\rho - \frac{c^2}{\cosh^2\rho}, \qquad h_{\rho\tau} = h_{\tau\rho} = 0. \tag{4.23}$$

This follows equally from eq. (4.22), eq. (4.12) or the Euclidean continuation of eq. (4.7).

Computing the action. As is familiar from the study of classical strings dual to Wilson loops without insertions [31, 45, 56, 57], the string action is not simply the Nambu-Goto or Polyakov action since the area of the minimal surface diverges as it approaches the Wilson contour on the boundary. One possible remedy in that context is to regularize the area by shifting the contour from $z = 0$ to $z = \epsilon$, remove the divergent piece from the area that is proportional to the length of the contour as $\epsilon \to 0^+$, and interpret it as a renormalization of the mass of the particle moving around the loop [56, 57]. An alternative approach is to take the Legendre transform of the Nambu-Goto action with respect to the bulk radial coordinate [31]. This adds a boundary term to the string action that does not change the equations of motion or the extremal surface but does change the value of the action and makes it well-defined (and, when applicable, in agreement with gauge theory). We adopt this second approach for the computation of the action of the classical string dual to the

[20] One may also define the large charge vertex operators to be $v^J \equiv \lim_{\tau\to-\infty}(2g\sin\theta e^{i\phi}/z)^J$ and $\bar{v}^J \equiv \lim_{\tau\to\infty}(2g\sin\theta e^{-i\phi}/z)^J$, so that we send $\tau \to \mp\infty$ without sending $\rho \to \pm\infty$ first. The order of limits does not matter and the resulting classical vertex operators reproduce $v_{\rm cl}^J(-\varphi_L)$ and $\bar{v}_{\rm cl}^J(\varphi_L)$, as given by eq. (4.20).

JHEP03(2022)020

Wilson loop with insertions, but must modify the precise prescription in [31] to reflect the modified boundary conditions of the string arising from the insertions.

Because of its important role in what follows[21] let us briefly review the boundary term proposed in [31] for the classical string dual to a smooth Wilson loop without insertions. We call this the DGO boundary term, in reference to the authors' initials. We begin by combining the inverse bulk coordinate $u \equiv 1/z$ with the embedding coordinates Θ_I for S^5 into $u_I \equiv u\Theta_I$. This satisfies $u_I u_I = u^2$. In these coordinates, the metric on $\mathrm{EAdS}_5 \times S^5$ can be written

$$ds^2 = u^2 dx^\mu dx_\mu + \frac{du^2}{u^2} + d\Theta_I d\Theta_I = u^2 dx^\mu dx_\mu + \frac{du_I du_I}{u^2}. \tag{4.24}$$

Then the induced metric on the worldsheet is $h_{\alpha\beta} = u^2 \partial_\alpha x^\mu \partial_\beta x_\mu + u^{-2} \partial_\alpha u_I \partial_\beta u_I$, and we define the canonical momenta conjugate to u_I and u to be

$$\Pi_I^\alpha \equiv 2g \frac{\partial\sqrt{h}}{\partial(\partial_\alpha u_I)} = \frac{2g}{u^2}\sqrt{h}h^{\alpha\beta}\partial_\beta u_I, \qquad \Pi_u^\alpha \equiv 2g \frac{\partial\sqrt{h}}{\partial(\partial_\alpha u)} = \frac{2g}{u^2}\sqrt{h}h^{\alpha\beta}\partial_\beta u. \tag{4.25}$$

In this language, the DGO prescription is to take the Legendre transform with respect to u or, equivalently, with respect to the u_I by adding to the Nambu-Goto action the following boundary action:

$$S_{\mathrm{DGO}}[\Psi] = -\int d^2\sigma \partial_\alpha (u\Pi_u^\alpha) = -\int d^2\sigma \partial_\alpha (u_I \Pi_I^\alpha). \tag{4.26}$$

The variation of the Nambu-Goto action plus the DGO action under $u_I \to u_I + \delta u_I$ about a classical solution is then

$$\delta S_{\mathrm{NG}}[\Psi_{\mathrm{classical}}] + \delta S_{\mathrm{DGO}}[\Psi_{\mathrm{classical}}] = -\int d^2\sigma \partial_\alpha \left(u_I \delta\Pi_I^\alpha\right). \tag{4.27}$$

For the variation to be zero, we must send $\delta\Pi_I^\alpha \to 0$ at the boundary of the worldsheet, which means the complete action is to be viewed as a functional of the momentum Π_I instead of the coordinates u_I at the boundary. The DGO boundary term can therefore be thought of as imposing Neumann, rather than Dirichlet, boundary conditions on u_I.[22]

As a simple check of eq. (4.26), we compute the action of the string with $c = 0$, which is dual to the half-BPS Wilson loop without insertions. In this case $\sqrt{h} = \cosh\rho$, $\partial_\rho(u\Pi_u^\rho) = 2g\cosh\rho$, and $\partial_\tau(u\Pi_u^\tau) = 2g\,\mathrm{sech}^2\tau\,\mathrm{sech}\,\rho$, which reproduces the well known result

$$S_{\mathrm{NG}}[\Psi_{\mathrm{cl}}(0)] + S_{\mathrm{DGO}}[\Psi_{\mathrm{cl}}(0)] = -2g\int d\tau d\rho\,\mathrm{sech}\,\rho\,\mathrm{sech}^2\tau = -4\pi g. \tag{4.28}$$

This is just the string tension, $2g$, times the regularized area of EAdS_2, -2π, and matches the leading behavior of the gauge theory result in the supergravity regime given in eq. (2.2).

[21] There also appears to be a subtle issue with a minus sign in the original discussion [31]. We thank Nadav Drukker for correspondence on this detail.

[22] This in turn is equivalent to imposing Dirichlet conditions on the Θ^I, see [31], which is just the familiar statement that the coupling to the scalars in the Wilson loop sets the boundary values of the S^5 coordinates of the dual string.

JHEP03(2022)020

Our characterization of the boundary term in eq. (4.26) closely follows the one in [31] except that the original discussion was framed in terms of z and $Y_I \equiv z\Theta_I$, and the momenta $\Pi^\alpha_z \equiv \frac{2g}{z^2}\sqrt{h}h^{\alpha\beta}\partial_\beta z$ and $\Pi^\alpha_{Y_I} \equiv \frac{2g}{z^2}\sqrt{h}h^{\alpha\beta}\partial_\beta Y_I$. But since $z\Pi^\alpha_z = -u\Pi^\alpha_u$ and $Y_I\Pi^\alpha_{Y_I} = -u_I\Pi^\alpha_I$, the DGO boundary term expressed in terms of the z and Y_I coordinates does not have the minus sign in eq. (4.26). Therefore, in contrast with eq. (4.27), the variation about a classical solution of the Nambu-Goto action plus DGO boundary term under $Y^I \to Y^I + \delta Y^I$ does not vanish when the momenta $\Pi^\alpha_{Y_I}$ conjugate to Y^I are fixed at the boundary. For this reason, the DGO term should be viewed as a Legendre transform in u, not z, or in u_I, not Y^I.

Finally, we are ready to propose a precise form for $S_{\rm bdy}[\Psi]$ and evaluate the action. We begin with a few motivating observations. First, the vertex operators in eq. (4.15) are naturally written in terms of u_4 and u_5 as $v \equiv 2g\lim_{\rho\to\eta\infty}(u_4 + iu_5)$ and $\bar{v} \equiv 2g\lim_{\rho\to\eta\infty}(u_4 - iu_5)$. Secondly, the limiting behavior of $u_4 \pm iu_5$ evaluated on the classical solution, eq. (4.22), as the string approaches the insertions is

$$\lim_{\tau\to-\infty} u_4 + iu_5 = \frac{ce^{i\phi_0}}{2}, \qquad \lim_{\tau\to\infty} u_4 - iu_5 = \frac{ce^{-i\phi_0}}{2}. \tag{4.29}$$

These limits are taken with ρ fixed but general. Finally, the limiting behavior of the momenta conjugate to $u_4 \pm iu_5$, $\Pi^\alpha_{4\pm i5} \equiv \frac{1}{2}(\Pi^\alpha_4 \mp i\Pi^\alpha_5)$, evaluated on the classical solution is

$$\lim_{\tau\to-\infty} \Pi_{4-i5} = 0, \qquad \lim_{\tau\to\infty} \Pi_{4+i5} = 0. \tag{4.30}$$

By contrast, $u_4 + iu_5$ and $u_4 - iu_5$ diverge as $\tau \to \infty$ and $\tau \to -\infty$, respectively and Π_{4-i5} and Π_{4+i5} approach non-trivial functions of ρ as $\tau \to \infty$ and $\tau \to -\infty$, respectively.[23]

Eqs. (4.29) and (4.30) indicate that, as compared to the general prescription in [31], inserting Z^J and $\bar{Z}^J$ on the Wilson loop changes the boundary condition of $u_4 + iu_5$ at $\tau \to -\infty$ and of $u_4 - iu_5$ at $\tau \to \infty$ from Neumann to Dirichlet. We therefore propose that the correct boundary action is the DGO action in eq. (4.26), except with the Legendre transformation on $u_4 \pm iu_5$ at $\tau = \mp\infty$ removed:

$$S_{\rm bdy}[\Psi] \equiv S_{\rm DGO}[\Psi] - \int d\rho \lim_{\tau\to-\infty}(u_4 + iu_5)\Pi^\tau_{4+i5} + \int d\rho \lim_{\tau\to\infty}(u_4 - iu_5)\Pi^\tau_{4-i5}. \tag{4.31}$$

Like the Nambu-Goto action, this boundary action is not finite by itself. The bulk and boundary actions should be added as in eq. (4.16) with IR cutoffs imposed on both ρ and τ, and the sum then approaches a finite value as the cutoffs are removed.

The evaluation of the complete action is now simple, especially using the coordinates in eq. (4.22). Firstly, we note

$$(u_4 + iu_5)\Pi^\tau_{4+i5} = \frac{\tanh\tau - 1}{2}\Pi_\phi, \qquad (u_4 - iu_5)\Pi^\tau_{4-i5} = \frac{\tanh\tau + 1}{2}\Pi_\phi, \tag{4.32}$$

where Π_ϕ is the angular momentum density introduced in eq. (4.9). The second two terms in eq. (4.31) therefore evaluate to

$$-\int d\rho \lim_{\tau\to-\infty}(u_4 + iu_5)\Pi^\tau_{4+i5} = \int d\rho \lim_{\tau\to\infty}(u_4 - iu_5)\Pi^\tau_{4-i5} = \int d\rho\Pi_\phi = J. \tag{4.33}$$

[23] Specifically, $\lim_{\tau\to\infty}\Pi^\alpha_{4-i5} = -\lim_{\tau\to-\infty}\Pi^\alpha_{4+i5} = 4gc/\cosh^2\rho/\sqrt{\cosh^2\rho - c^2}\delta^{\tau\alpha}$.

JHEP03(2022)020

Furthermore, one can check that the ρ term in the DGO Lagrangian satisfies $\partial_\rho(u\Pi^\rho_u) = 2g\sqrt{h}$ and therefore cancels with the Nambu-Goto Lagrangian, while the τ term simplifies to $\partial_\tau(u\Pi^\tau_u) = 2g\,\mathrm{sech}^2\,\tau/\sqrt{\cosh^2\rho - c^2}$. Therefore,

$$\begin{aligned} S_{\mathrm{NG}}[\Psi_{\mathrm{cl}}(c)] + S_{\mathrm{DGO}}[\Psi_{\mathrm{cl}}(c)] &= -2g\int_{-\infty}^{\infty}\frac{d\tau}{\cosh^2\tau}\int_{-\infty}^{\infty}\frac{d\rho}{\sqrt{\cosh^2\rho - c^2}} \\ &= -8g\mathbb{K}(c^2). \end{aligned} \tag{4.34}$$

Combined with eq. (4.33) and recalling eq. (4.9), we determine the complete action of the classical string to be

$$S_{\mathrm{cl}}(c) = S_{\mathrm{NG}} + S_{\mathrm{bdy}} = -8g\mathbb{K}(c^2) + 2J = -8g\mathbb{E}(c^2). \tag{4.35}$$

Then, from eq. (4.19) and including the contribution of the vertex operators eq. (4.21), we obtain the two-point function

$$\langle\langle Z^J(-\varphi_L)\bar{Z}^J(\varphi_L)\rangle\rangle = \frac{(2gc)^{2J}}{d^{2J}}e^{8g\mathbb{E}(c^2)-8g\mathbb{E}(0)}. \tag{4.36}$$

Note that if we put Z^J and $\bar{Z}^J$ in the topological configuration by sending $\varphi_L \to \pi/2$, as in eq. (2.19), we find

$$\langle\langle\tilde{\Phi}^J\tilde{\Phi}^J\rangle\rangle = (-g^2c^2)^J e^{8g\mathbb{E}(c^2)-8g\mathbb{E}(0)}. \tag{4.37}$$

This is in precise agreement with the localization result in eq. (3.57).

We should emphasize that although we have for simplicity written the boundary action eq. (4.31) using the global coordinates ρ and τ, the complete action is independent of the choice of worldsheet coordinates and IR regularization.[24]

Before proceeding to the computation of the higher-point functions, we close this section with some comments about the evaluation of the string action. We begin by noting, since $d\mathbb{E}(c^2)/dc = (\mathbb{K}(c^2) - \mathbb{E}(c^2))/c$, that the two-point function is extremized with respect to c:

$$\frac{\partial}{\partial c}\left(2J\log c + S_{\mathrm{cl}}(c)\right)\Big|_{c=c(J)} = 0. \tag{4.39}$$

[24]This can be seen as follows. Firstly, the sum of the Nambu-Goto and DGO actions is manifestly worldsheet reparametrization invariant and one can also readily check that it is finite without need for regularization. Secondly, the first boundary term in eq. (4.31) can be written in a coordinate independent way as follows (the treatment of the second boundary term is analogous):

$$-\int d\rho \lim_{\tau\to-\infty}(u_4 + iu_5)\Pi^\tau_{4+i5} = -\lim_{\Lambda\to\infty}\int_{\eta_\Lambda} d\lambda\sqrt{\gamma}n_\alpha P^\alpha. \tag{4.38}$$

Here, η_Λ is a family of curves that approach Z^J as $\Lambda\to\infty$, λ is a coordinate along η_Λ that we may for concreteness take to run from -1 to 1, $\gamma_{\alpha\beta} \equiv \frac{d\eta^\alpha}{d\lambda}\frac{d\eta^\beta}{d\lambda}h_{\alpha\beta}$ is the induced metric on η_Λ, n_α is a unit normal vector (i.e., $\frac{d\eta^\alpha}{d\lambda}n_\alpha = 0$ and $n_\alpha n_\beta h^{\alpha\beta} = 1$), and finally $P^\alpha \equiv (u_4 + iu_5)\Pi^\alpha_{4+i5}/\sqrt{h}$. The point, then, is that the limit on the r.h.s. of eq. (4.38) is independent of the particular choice of $\eta_\Lambda(\lambda) \equiv (\rho_\Lambda(\lambda), \tau_\Lambda(\lambda))$ as long as $\rho_\Lambda(+1)\to\infty$, $\rho_\Lambda(-1)\to-\infty$ and $\max_{\lambda\in[-1,1]}\tau_\Lambda(\lambda)\to-\infty$ as $\Lambda\to\infty$, which is what we mean when we say that η_Λ "approaches Z^J" as $\Lambda\to\infty$.

JHEP03(2022)020

Here, we treat c and J as independent variables when taking the partial derivative, and $c(J)$ is the particular value of c satisfying eq. (4.9). If we view the vertex operators in eq. (4.14) as additional boundary terms in a "total" action,

$$S_{\text{tot}}[\Psi] \equiv -J \log \left(v(-\varphi_L; \Psi) \bar{v}(\varphi_L; \Psi) \right) + S[\Psi], \tag{4.40}$$

then eq. (4.39) is equivalent to

$$\left. \frac{\partial S_{\text{tot}}[\Psi_{\text{cl}}(c)]}{\partial c} \right|_{c=c(J)} = 0 \,. \tag{4.41}$$

This tells us that the total action is invariant when we vary θ by $\delta\theta = \delta c / \sqrt{\cosh^2 \rho - c(J)^2}$ about the classical string solution, which is equivalent to varying c by δc about $c(J)$, as we would expect from a purportedly extremal solution. By contrast, the Nambu-Goto action plus the DGO action without the additional two terms in eq. (4.31), which evaluates to eq. (4.34) on the classical string, does not satisfy this extremization property. Therefore, we may say that modifying the boundary conditions of $u_4 + iu_5$ and $u_4 - iu_5$ to be Dirichlet instead of Neumann at $\tau \to -\infty$ and $\tau \to \infty$, respectively— and implementing the necessary Legendre transforms with the boundary action given in eq. (4.31)— fixes the θ variational problem, which would otherwise not be well defined.[25]

Requiring the θ variational problem to be well defined does not uniquely determine $S_{\text{bdy}}[\Psi]$. For example, the boundary terms in the DGO action implementing the Legendre transforms of u_1, u_2, and u_3 at $\tau \to \pm\infty$ are all zero because $\Theta_1 = \Theta_2 = \Theta_3 = 0$ on the string solution. And given eq. (4.32), the same is true for the two terms implementing the Legendre transforms of $u_4 + iu_5$ at $\tau \to \infty$ and of $u_4 - iu_5$ at $\tau \to -\infty$. Any of these terms may therefore be dropped without changing the value of the action. Thus, our findings do not rule out the possibility that the correct boundary prescription is to also impose Dirichlet conditions on u_1, u_2, and u_3 at $\tau \to \pm\infty$, and/or perhaps on $u_4 + iu_5$ at $\tau \to \infty$ and $u_4 - iu_5$ at $\tau \to -\infty$. However, we consider the boundary conditions we identified and the boundary action given in eq. (4.31) to be the most plausible. Our proposal could be further tested by applying it to a more general string solution in which the behavior of the S^5 directions orthogonal to the large charge directions is not trivial. One possibility is to study the semiclassical string dual to the quarter-BPS Wilson loop [58] with Z^J and $\bar{Z}^J$ additionally inserted.

Next, it is instructive to compare the behavior of eq. (4.36) in the limit $\mathcal{J} \to \infty$ to the results in [30]. Noting that $2\mathcal{J} \log c \to 0$ and $\mathbb{E}(c^2) \to 1$ as $\mathcal{J} \to \infty$, we find that in the large $\mathcal{J}$ limit

$$\langle\langle Z^J(-\varphi_L) \bar{Z}^J(\varphi_L) \rangle\rangle = \frac{(2g)^{2J}}{d^{2J}} \exp\left[g \left(8 - 4\pi + O(\mathcal{J} e^{-\frac{\mathcal{J}}{2}}) \right) + O(g^0) \right]. \tag{4.42}$$

[25] Incidentally, eq. (4.39) uniquely determines $S_{\text{cl}}(c)$. It allows to completely bypass the detailed discussion of the boundary action and uses only the fact that the c dependence of the vertex operators goes like c^{2J} and that the variation of $S_{\text{tot}}[\Psi]$ about the classical string solution should vanish, including when we vary θ by varying c.

JHEP03(2022)020

Eq. (18) in [30] differs from our result above by an extra $2J$ in the exponent.[26] This is because the analysis in [30] used the DGO boundary action in eq. (4.26) instead of the modified boundary action in eq. (4.31). We have seen that this difference in choice of boundary term indeed changes the action by $2J$.

Finally, it is interesting to compare our analysis of the classical string dual to large charges Z^J and $\bar{Z}^J$ inserted *on* the Wilson loop to the string calculation of the correlation function of the Wilson loop and a large charge single-trace local operator $\mathrm{tr}Z^J$ inserted *away from* the Wilson loop [38, 40, 59]. The classical string solution in that case is topologically a cone whose boundary is the disjoint union of a point incident on the local insertion and a circle incident on the Wilson loop. Our analysis is most directly similar to the one in [59], where the action is also computed with a DGO boundary term added to the Nambu-Goto action.[27] In that paper, the DGO term is written not as a bulk integral of a total derivative like in eq. (4.26), which would give contributions from both boundaries, but rather as a boundary integral over only the boundary incident on the Wilson loop. Given our discussion above, we interpret this to mean that the u_I coordinates satisfy Neumann conditions on the boundary incident on the Wilson loop, as in the DGO prescription, but Dirichlet conditions on the boundary incident on the local insertion.[28] Moreover, if we instead write the DGO term in [59] as a bulk integral of a total derivative or equivalently add the DGO term also for the boundary incident on the local operator, then we find the action changes by J, just like in eq. (4.33). Thus, the semiclassical string analysis of Z^J and $\bar{Z}^J$ inserted on the Wilson loop is very similar to the analysis of $\mathrm{tr}Z^J$ inserted away from the Wilson loop, except that splitting the boundary of the string worldsheet into a part incident on the local insertions and a part incident on the Wilson loop proper is more subtle in the former case.

4.3 Higher-point functions

The procedure we used to compute the large charge limit of the two-point function can be straightforwardly extended to higher-point functions. For every extra insertion of $Z^\ell(\varphi)$ in the Wilson loop correlator, we simply add an extra factor of $v_{\mathrm{cl}}^\ell(\varphi)$ in the integral over ϕ_0

[26] Specifically, eq. (18) in [30] gives the following value for the total action (including the contributions from the vertex operators):

$$S_{\mathrm{tot}} = 2J \log \frac{2\ell}{\epsilon} - 2J - \frac{2R^2}{\pi\alpha'}.$$

Identifying $2\ell \to d$ as the distance between the insertions, $\frac{R^2}{2\pi\alpha'} \to 2g$ as the string tension and ϵ as an IR regulator as $z \to 0$ that [30] imposed, we find that the above expression differs from the negative log of eq. (4.42) by $2J + 4\pi g + 2J \log \frac{\epsilon}{2g}$. The $4\pi g$ and $2J \log \frac{\epsilon}{2g}$ terms in the difference arise because, unlike [30], we normalize the Wilson loop with insertions by the Wilson loop without insertions (see eqs. (2.4) and (4.14)) and we include a factor of $2g/z$ in the vertex operators as we approach the boundary (see eq. (4.15)). Accounting for these differences in convention, the substantive difference between the two results is therefore simply $2J$.

[27] [38, 40] used different, equivalent methods to regulate the semiclassical action.

[28] More precisely, we would say that the combination of the u_I coordinates dual to Z satisfies the Dirichlet condition on the insertion. The other linear combinations should still satisfy Neumann conditions but the boundary terms implementing their Legendre transforms evaluate to zero and can effectively be dropped.

JHEP03(2022)020

in eq. (4.19), and likewise for $\bar{Z}^\ell(\varphi)$ and $\bar{v}_{\rm cl}^\ell(\varphi)$. Thus, in the large charge limit,

$$\begin{aligned}\frac{\langle\langle Z^J(-\varphi_L)\bar{Z}^J(\varphi_L)\prod_{i=1}^n Z^{\ell_i}(\varphi_i)\prod_{j=1}^m \bar{Z}^{\bar{\ell}_j}(\bar{\varphi}_j)\rangle\rangle}{\langle\langle Z^J(-\varphi_L)\bar{Z}^J(\varphi_L)\rangle\rangle}&\\ = \frac{1}{2\pi}\int_0^{2\pi} d\phi_0 \prod_{i=1}^n v_{\rm cl}^{\ell_i}(\varphi_i)\prod_{j=1}^m \bar{v}_{\rm cl}^{\bar{\ell}_j}(\bar{\varphi}_j)&\\ = \frac{(2gc)^{2\ell_{\rm tot}} d^{2\ell_{\rm tot}}}{\prod_{i=1}^n d(\varphi_i,\varphi_L)^{2\ell_i}\prod_{j=1}^m d(\bar{\varphi}_j,-\varphi_L)^{2\bar{\ell}_j}}\delta_{\ell_{\rm tot},\bar{\ell}_{\rm tot}}.&\end{aligned} \tag{4.43}$$

Here, we let $\ell_{\rm tot}\equiv\sum_{i=1}^n \ell_i$ and $\bar{\ell}_{\rm tot}\equiv\sum_{j=1}^m \bar{\ell}_j$.

We could also be interested in higher-point functions in which the light operators are not just finite powers of Z and $\bar{Z}$. However, the orthogonal scalars Φ_1, Φ_2 and Φ_3 are effectively "invisible" in the large charge limit, as is clear from the perspective of the dual string: since $\Theta_i = 0$ for $i = 1, 2, 3$ on the classical string solution, the corresponding classical vertex operators, $\lim_{\rm bulk\to bdy}\Theta_i/z$, are trivially zero. This means that correlators involving light operators of the form $(\epsilon\cdot\Phi)^\ell$, where $\epsilon\cdot\Phi = \epsilon_1\Phi_1+\epsilon_2\Phi_2+\epsilon_3\Phi_3+\epsilon_Z Z+\epsilon_{\bar{Z}}\bar{Z}$, reduce to linear combinations of the correlators in eq. (4.43) after the truncation $\epsilon\cdot\Phi\to\epsilon_Z Z+\epsilon_{\bar{Z}}\bar{Z}$. Alternatively, we can compute correlators of the more general light operators directly using the classical string by replacing $\epsilon\cdot\Phi$ in the Wilson loop correlator with $\epsilon_Z v_{\rm cl}+\epsilon_{\bar{Z}}\bar{v}_{\rm cl}$ in the integral over ϕ_0. (The correlators resulting from such truncation may of course be zero, like when $\epsilon_Z=\epsilon_{\bar{Z}}=0$, in which case we need to go beyond the classical analysis to determine the leading non-trivial contribution. For instance, to determine the four-point correlator $\langle\langle Z^J\bar{Z}^J\Phi_1\Phi_1\rangle\rangle$, we need to study fluctuations of the semiclassical string, which will be discussed in [29].)

As a special case, we will compute the higher-point topological correlator in eq. (2.14). Firstly, we again set $\varphi_L = \pi/2$ to put the large charges in the topological configuration. The light vertex operators then simplify to $v_{\rm cl}(\varphi) = 2gce^{i\phi_0}/(1-\sin\varphi)$ and $\bar{v}_{\rm cl}(\varphi) = 2gce^{-i\phi_0}/(1+\sin\varphi)$. Furthermore, since $\tilde{\Phi}^\ell(\varphi) = \left(\cos\varphi\Phi_3 + \left(\frac{1-\sin\varphi}{2}\right)Z - \left(\frac{1+\sin\varphi}{2}\right)\bar{Z}\right)^\ell$, the light vertex operators for the topological operators on the classical string are manifestly position independent:

$$\tilde{\Phi}^\ell \to \left(\frac{1-\sin\varphi}{2}v_{\rm cl}(\varphi)+\frac{1+\sin\varphi}{2}\bar{v}_{\rm cl}(\varphi)\right)^\ell = (gc)^\ell\left(e^{i\phi_0}-e^{-i\phi_0}\right)^\ell. \tag{4.44}$$

Therefore, eq. (2.14) becomes

$$\frac{\langle\langle\tilde{\Phi}^J\tilde{\Phi}^J\prod_{i=1}^n\tilde{\Phi}^{\ell_i}\rangle\rangle}{\langle\langle\tilde{\Phi}^J\tilde{\Phi}^J\rangle\rangle} = \frac{(gc)^{\ell_{\rm tot}}}{2\pi}\int_0^{2\pi} d\phi_0 (e^{i\phi_0}-e^{-i\phi_0})^{\ell_{\rm tot}}. \tag{4.45}$$

Here, we again have defined $\ell_{\rm tot}\equiv\sum_{i=1}^n\ell_i$. If we expand the integrand using the binomial theorem, the only term that does not integrate to zero has equal numbers of $e^{i\phi_0}$ and $e^{-i\phi_0}$. Thus, the integral counts the number of ways of grouping $\ell_{\rm tot}$ objects into two equal halves, and the correlator simplifies to

$$\frac{\langle\langle\tilde{\Phi}^J\tilde{\Phi}^J\prod_{i=1}^n\tilde{\Phi}^{\ell_i}\rangle\rangle}{\langle\langle\tilde{\Phi}^J\tilde{\Phi}^J\rangle\rangle} = (-g^2c^2)^{\ell_{\rm tot}/2}\binom{\ell_{\rm tot}}{\ell_{\rm tot}/2}. \tag{4.46}$$

This matches the localization result in eq. (3.40).

JHEP03(2022)020

We can also extend the analysis to correlators involving two large operators with unequal charges J and $J+\ell$, where ℓ is held fixed in the large charge limit. The string path integral is dominated by the same saddle point, $\Psi \to \Psi_{\rm cl}(c(J))$, and therefore the classical action and the vertex operators are the same as before.[29] The only difference is that the classical vertex operator for the $J+\ell$ charge has ℓ extra copies of $v_{\rm cl}(-\varphi_L)$. For instance, the generalization of eq. (4.43) is

$$\begin{aligned}\frac{\langle\langle Z^{J+\ell}(-\varphi_L)\bar{Z}^J(\varphi_L)\prod_{i=1}^n Z^{\ell_i}(\varphi_i)\prod_{j=1}^m \bar{Z}^{\bar{\ell}_j}(\bar{\varphi}_j)\rangle\rangle}{\langle\langle Z^J(-\varphi_L)\bar{Z}^J(\varphi_L)\rangle\rangle} \\ = \frac{1}{2\pi}\int_0^{2\pi} d\phi_0 v_{\rm cl}^{\ell}\left(-\frac{\varphi_L}{2}\right)\prod_{i=1}^n v_{\rm cl}^{\ell_i}(\varphi_i)\prod_{j=1}^m \bar{v}_{\rm cl}^{\bar{\ell}_j}(\bar{\varphi}_j) \\ = \frac{(2gc)^{\ell_{\rm tot}+\bar{\ell}_{\rm tot}+\ell} d^{\ell_{\rm tot}+\bar{\ell}_{\rm tot}-\ell}}{\prod_{i=1}^n d(\varphi_i,\varphi_L)^{2\ell_i}\prod_{j=1}^m d(\bar{\varphi}_j,-\varphi_L)^{2\bar{\ell}_j}}\delta_{\ell_{\rm tot}+\ell,\bar{\ell}_{\rm tot}}.\end{aligned} \tag{4.47}$$

Furthermore, to determine the corresponding topological correlators, we again set $\varphi_L = \pi/2$, replace $\tilde{\Phi}^{J+\ell} \to v_{\rm cl}(-\frac{\pi}{2})^{J+\ell} = (gc)^{J+\ell}e^{i(J+\ell)\phi_0}$ and $\tilde{\Phi}^J \to (-1)^J\bar{v}(\frac{\pi}{2})^J = (-gc)^J e^{-iJ\phi_0}$ for the heavy operators and use eq. (4.44) for the light operators. This yields

$$\begin{aligned}\frac{\langle\langle \tilde{\Phi}^{J+\ell}\tilde{\Phi}^J\prod_{i=1}^n\tilde{\Phi}^{\ell_i}\rangle\rangle}{\langle\langle\tilde{\Phi}^J\tilde{\Phi}^J\rangle\rangle} &= \frac{(gc)^{\ell_{\rm tot}+\ell}}{2\pi}\int_0^{2\pi} d\phi_0 e^{i\ell\phi_0}(e^{i\phi_0}-e^{-i\phi_0})^{\ell_{\rm tot}} \\ &= (-g^2c^2)^{\frac{\ell_{\rm tot}+\ell}{2}}\binom{\ell_{\rm tot}}{(\ell_{\rm tot}-\ell)/2},\end{aligned} \tag{4.48}$$

which indeed reduces to eq. (4.46) when $\ell = 0$. One consequence of eqs. (4.46) and (4.48) is that $\tilde{\Phi}^{\ell_1}\tilde{\Phi}^{\ell_2}$ and $\tilde{\Phi}^{\ell_1+\ell_2}$ are equal in the large charge limit, but $\tilde{\Phi}^{J+\ell}$ and $\tilde{\Phi}^J\tilde{\Phi}^\ell$ are not.

As a simple check of eq. (4.48), we note that when $\ell = \ell_{\rm tot}$ it reproduces the leading behavior of $\langle\tilde{\Phi}^{J+\ell}\tilde{\Phi}^{J+\ell}\rangle / \langle\tilde{\Phi}^J\tilde{\Phi}^J\rangle$, which is given in eq. (3.80).[30] This is in accordance with the property of extremal correlators stated in eq. (3.64). It also follows that, if we use eq. (4.48) to determine the normalized extremal OPE coefficient defined in eq. (3.78), then we reproduce the leading order term, $(g\pi c^2)^\ell/\ell!$, in eq. (3.82). This normalized OPE coefficient can alternatively be extracted from a simple conformal block calculation, as we'll see next.

CFT data from a four-point function. The final correlator we consider is the non-topological correlator with two equal large charges and two equal light charges. This is a

[29] We could also alternatively localize the path integral to $\Psi \to \Psi_{\rm cl}(c(J'))$ for any $J' = J + O(g^0)$, including $J' = J+\ell$. The resulting string correlators, now with vertex operators $v_{\rm cl}, \bar{v}_{\rm cl} \propto c(J')$ and action $S_{\rm cl}(c(J'))$, have the same leading behavior in the large charge limit. This follows from eq. (4.41). The analogous statement for the one-dimensional Laplace integral $\int e^{-Nf(x)}g(x)dx$, with N large and f minimized at x_0, is that the leading term $e^{-Nf(x_0)}g(x_0)$ is invariant under $x_0 \to x_0 + a/N$ because $f'(x_0) = 0$. See also the next footnote.

[30] The leading term in eq. (3.80) can also be deduced using only results from the dual string. Firstly, given eq. (3.79), we see that $c(J)^\ell = c(J+\ell)^\ell(1+O(1/g))$ for finite ℓ. Also, it follows from eq. (4.39) that $c(J)^{2J}e^{-S_{\rm cl}(c(J))} = c(J+\ell)^{2J}e^{-S_{\rm cl}(c(J+\ell))}(1+O(1/g))$. Applying these to eq. (4.37) implies $\langle\tilde{\Phi}^{J+\ell}\tilde{\Phi}^{J+\ell}\rangle = (-g^2c(J)^2)^\ell\langle\tilde{\Phi}^J\tilde{\Phi}^J\rangle(1+O(1/g))$, which is the desired result.

JHEP03(2022)020

special case of eq. (4.43) and is given by

$$\frac{\langle\langle Z^J(-\varphi_L)\bar{Z}^J(\varphi_L)Z^\ell(\varphi)\bar{Z}^\ell(\bar{\varphi})\rangle\rangle}{\langle\langle Z^J(-\varphi_L)\bar{Z}^J(\varphi_L)\rangle\rangle} = (2gc)^{2\ell}\frac{d(-\varphi_L,\varphi_L)^{2\ell}}{d(\varphi,\varphi_L)^{2\ell}d(\bar{\varphi},-\varphi_L)^{2\ell}}. \tag{4.49}$$

This four point function contains some simple large charge CFT data. We choose to study the conformal block expansion in the $Z^\ell Z^J \to \bar{Z}^\ell\bar{Z}^J$ channel, so that the smallest exchanged operators also have large charges. (By contrast, the smallest operators exchanged in the $Z^\ell\bar{Z}^\ell \to Z^J\bar{Z}^J$ channel are light).

Therefore, let us map $\varphi \to \varphi_1$, $\bar{\varphi} \to \varphi_3$, $-\varphi_L \to \varphi_2$ and $\varphi_L \to \varphi_4$, and assume for simplicity that $-\pi < \varphi_1 < \varphi_2 < \varphi_3 < \varphi_4 < \pi$. The four point function can be written

$$\langle\langle Z(\varphi_1)Z^J(\varphi_2)\bar{Z}(\varphi_3)\bar{Z}^J(\varphi_4)\rangle\rangle = \frac{(2gc)^{2(J+\ell)}e^{-S_{\rm cl}(c)}}{(d_{21}d_{43})^{J+\ell}}\left(\frac{d_{31}}{d_{42}}\right)^{J-\ell}\frac{\chi^{J+\ell}}{(1-\chi)^{2\ell}}, \tag{4.50}$$

where we have introduced the conformally invariant cross ratio, χ:

$$\chi \equiv \frac{d_{21}d_{43}}{d_{31}d_{42}}, \qquad \frac{\chi}{1-\chi} = \frac{d_{21}d_{43}}{d_{41}d_{32}}, \qquad \frac{1}{1-\chi} = \frac{d_{31}d_{42}}{d_{41}d_{32}}. \tag{4.51}$$

(4.50) is in a form that is convenient for comparing with the conformal block expansion [60],

$$\begin{aligned}&\langle\langle Z(\varphi_1)Z^J(\varphi_2)\bar{Z}(\varphi_3)\bar{Z}^J(\varphi_4)\rangle\rangle \\ &\quad= \frac{1}{(d_{21}d_{43})^{J+\ell}}\left(\frac{d_{31}}{d_{42}}\right)^{J-\ell}\sum_n p_n\chi^{\Delta_n}{}_2F_1(\Delta_n+\ell-J,\Delta_n+J-\ell,2\Delta_n,\chi).\end{aligned} \tag{4.52}$$

Here, $n = 0, 1, 2, \ldots$ labels the nth operator $\mathcal{O}_n$ appearing in the OPE of ZZ^J (and its conjugate $\bar{\mathcal{O}}_n$ appearing in the OPE of $\bar{Z}\bar{Z}^J$), Δ_n is the dimension of $\mathcal{O}_n$ (and $\bar{\mathcal{O}}_n$), $\chi^\Delta{}_2F_1(\chi)$ is the conformal block in one dimension and p_n is the nth conformal block coefficient.

The operators $\mathcal{O}_n$ in the OPE of Z and Z^J have dimensions of order J or higher. Therefore, two of the three parameters of the hypergeometric function are large, in which case it takes a simplified form [61]:

$${}_2F_1(\alpha, L+\beta, L+\gamma, \chi) = \frac{1}{(1-\chi)^\alpha}\left(1+O\left(\frac{1}{L}\right)\right). \tag{4.53}$$

Letting $L = 2J$, $\alpha = \Delta_n + \ell - J$, $\beta = \Delta_n - \ell - J$, $\gamma = 2(\Delta_n - J)$, we see that the leading behavior of the conformal block in eq. (4.52) is $\chi^{\Delta_n}/(1-\chi)^{\Delta_n+\ell-J}$. Then, matching eqs. (4.50) and (4.52), we find that there is only one operator, $\mathcal{O}_0$, contributing to the conformal block expansion in the large charge regime, and that its dimension and conformal block coefficient are:

$$\Delta_0 = J + \ell, \qquad p_0 = (2gc)^{2(J+\ell)}e^{-S_{\rm cl}(c)}. \tag{4.54}$$

We identify $\mathcal{O}_0 = \bar{Z}^{J+\ell}$, $\bar{\mathcal{O}}_0 = Z^{J+\ell}$, which have the right dimension. Additionally, the conformal block coefficient p_0 is related to the OPE coefficient for the three-point function $ZZ^J\bar{Z}^{J+\ell}$ and the normalization of the two-point function $Z^{J+\ell}\bar{Z}^{J+\ell}$, which up to factors of 2 coming from the polarization vectors of Z and $\bar{Z}$ are given by $c_{J+\ell,J,\ell}$ and n_J. More

JHEP03(2022)020

precisely, $p_0 = 2^{J+\ell} c^2_{J+\ell,J,\ell}/n_{J+\ell}$. Then, combining eq. (4.54) with eq. (4.37) and eq. (3.81) we find,

$$\frac{c^2_{J+\ell,J,\ell}}{n_{J+\ell} n_J n_\ell} = \frac{p_0}{2^{J+\ell} n_J n_\ell} = \frac{(g\pi c^2)^\ell}{\ell!}. \tag{4.55}$$

This agrees at leading order with eq. (3.82).

4.4 Small and large $\mathcal{J}$

In this final section, we discuss the behavior of some of the large charge correlators we have computed when $\mathcal{J} \ll 1$ or $\mathcal{J} \gg 1$. We also compare them to the large g and small g perturbative results for the planar, finite charge correlators from [10, 12, 19].

Small $\mathcal{J}$. When $\mathcal{J} \ll 1$, $\mathcal{J}$ and c^2 are related by the Taylor series

$$\mathcal{J} = \pi c^2 + \frac{3\pi}{8} c^4 + O(c^6), \qquad\qquad c^2 = \frac{\mathcal{J}}{\pi} - \frac{3}{8}\frac{\mathcal{J}^2}{\pi^2} + O(\mathcal{J}^3). \tag{4.56}$$

The first few terms in the small $\mathcal{J}$ expansions of the two-point function in eq. (4.37) and the normalized extremal three-point function in eq. (3.82) are:

$$\langle\langle \tilde{\Phi}^J \tilde{\Phi}^J \rangle\rangle = (-g^2)^J \exp\left[g\left(\mathcal{J}\log\mathcal{J} - \mathcal{J}(1+\log\pi) - \frac{3\mathcal{J}^2}{16\pi} + O(\mathcal{J}^3)\right) + O(g^0)\right], \tag{4.57}$$

$$\begin{aligned}\frac{c^2_{J+\ell,J,\ell}}{n_{J+\ell} n_J n_\ell} &= g^\ell \left(\frac{\mathcal{J}^\ell}{\ell!} - \frac{3}{8\pi}\frac{\mathcal{J}^{\ell+1}}{(\ell-1)!} + O(\mathcal{J}^{\ell+2})\right) \\ &\quad + g^{\ell-1}\left(\frac{\ell+1}{2(\ell-1)!}\mathcal{J}^{\ell-1} - \frac{3}{16\pi}\frac{\ell(\ell+1)}{(\ell-1)!}\mathcal{J}^\ell + O(\mathcal{J}^{\ell+1})\right) + O(g^{\ell-2}).\end{aligned} \tag{4.58}$$

We recall that our matrix model in sections 3.1–3.2 and the dual string analysis in section 4.3 only determine the g^ℓ term in eq. (4.58). The $g^{\ell-1}$ term comes from the Bremsstrahlung analysis in 3.3.

The expansion of the large charge correlators in small $\mathcal{J}$ pushes results that are valid when $1 \ll J \sim g$ into the regime $1 \ll J \ll g$. This should agree with the expansion of finite charge correlators in large J, which pushes results that are valid when $1 \sim J \ll g$ also into the regime $1 \ll J \ll g$. More specifically, we expect the coefficient of the $g^{-m}\mathcal{J}^n$ term in the double expansion in $1/g$ and $\mathcal{J}$ to match the coefficient of the $g^{-m-n}J^n$ term in the double expansion in $1/g$ and $1/J$.[31]

Therefore, we can use the $1/g$ expansion of the finite J correlators, determined using localization in [12], to test eqs. (4.57)–(4.58). The two-point function (modulo eq. (2.11)) is given in eq. (3.81) and the three-point function is

$$\frac{c^2_{J+\ell,J,\ell}}{n_{J+\ell} n_J n_\ell} = \frac{(J+\ell)!}{J!\ell!}\left(1 - \frac{3}{8\pi}\frac{J\ell}{g} + O(1/g^2)\right). \tag{4.59}$$

[31] This is equivalent to saying that the mth sub-leading term in the $1/g$ expansion with finite $\mathcal{J}$ should equal the resummation of the $(m+1)$th largest J terms at each order in the $1/g$ expansion with finite J.

JHEP03(2022)020

Putting the two-point function in a form parallel to eq. (4.57) and then expanding in large J, we find

$$\begin{aligned}\langle\langle\tilde{\Phi}^J\tilde{\Phi}^J\rangle\rangle &= (-g^2)^J \exp\left[\log\frac{J!}{(g\pi)^J} - \frac{3}{32\pi g}(2J^2+J)+O(1/g^2)\right] \\ &= (-g^2)^J \exp\left[\left(J\log\frac{J}{g} - J(1+\log\pi)+O(J^0)\right) - \frac{1}{g}\left(\frac{3J^2}{16\pi}+O(J)\right)+O(1/g^2)\right]\end{aligned} \tag{4.60}$$

which matches eq. (4.57) in the overlapping terms. Likewise, expanding the three-point function in large J yields

$$\begin{aligned}\frac{c^2_{J+\ell,J,\ell}}{n_{J+\ell}n_J n_\ell} &= \left(\frac{J^\ell}{\ell!} + \frac{(\ell+1)J^{\ell-1}}{2(\ell-1)!} + O(J^{\ell-2})\right) \\ &\quad - \frac{1}{g}\left(\frac{3}{8\pi}\frac{J^{\ell+1}}{(\ell-1)!} + \frac{3}{16\pi g}\frac{\ell(\ell+1)J^\ell}{(\ell-1)!} + O(J^{\ell-1})\right) + O(1/g^2),\end{aligned} \tag{4.61}$$

which matches eq. (4.58) in the overlapping terms.

Eqs. (3.81) and (4.59) follow from localization, but may also be understood in terms of the EAdS$_2$ string dual to the Wilson loop without insertions. The leading strong coupling behavior of the finite charge correlators is determined by a free theory with boundary-to-boundary propagators [10]

$$\langle\Phi_I(\varphi_i)\Phi_J(\varphi_j)\rangle = \frac{2g}{\pi}\frac{\delta_{IJ}}{d_{ij}^2}, \tag{4.62}$$

where $I, J = 1, \ldots, 5$. For non-coincident insertions of the topological operators, the boundary propagator is $\langle\tilde{\Phi}\tilde{\Phi}\rangle = -g/\pi$. For Z and $\bar{Z}$, the boundary propagator is $\langle Z(\varphi_i)\bar{Z}(\varphi_j)\rangle = \frac{4g}{\pi}\frac{1}{d_{ij}^2}$, $\langle ZZ\rangle = \langle\bar{Z}\bar{Z}\rangle = 0$. In this language, the leading term in eq. (4.60) arises from the $J!$ ways to contract the two insertions of $\tilde{\Phi}^J$, and the leading term in $c_{J+\ell,J,\ell}$ in eq. (4.59) comes from the $\binom{J+\ell}{J}J!\ell!$ ways to contract J fields in $\tilde{\Phi}^{J+\ell}$ with $\tilde{\Phi}^J$ and the remaining ℓ fields in $\tilde{\Phi}^{J+\ell}$ with $\tilde{\Phi}^\ell$.[32]

Using the EAdS$_2$ free theory, we can similarly determine the leading strong coupling behavior of eq. (4.43) when J is finite. This serves as a check of the large charge result, including the position dependence. The general expression resulting from summing all possible boundary-to-boundary contractions between the Z and $\bar{Z}$ insertions in the numerator of eq. (4.43) is rather cumbersome. However, to compare with the large charge result in eq. (4.43), we only need the contribution with the largest power of J, which comes from the diagrams where the light operators are contracted only with the heavy operators, and the remaining fields of the heavy operators are contracted with each other; see figure 6. The number of such contractions is $J!^2/(J-\ell_{\text{tot}})!$. After dividing by $\langle Z^J\bar{Z}^J\rangle = J!\left(\frac{4g}{\pi d^2}\right)^J$, and

[32] It is also possible to reproduce the next-to-leading order terms by considering fluctuations of the EAdS$_2$ string and including the contribution of the four-point contact diagram with an interaction in the bulk that was studied in [10]. However, we stick to the free theory analysis both for simplicity and because it is sufficient for the purpose of checking leading large charge behavior.

JHEP03(2022)020

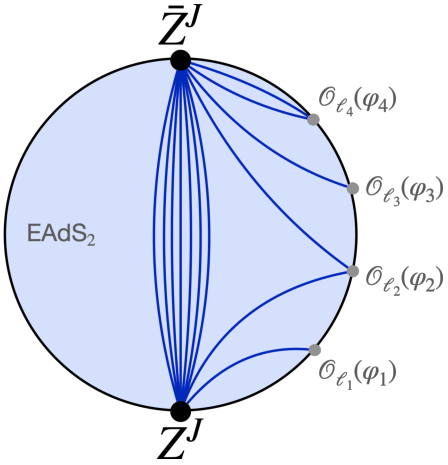

Figure 6. In the planar and strongly coupled regime, the leading behavior (in $1/g$) of the defect correlators of operators with parametrically small charges can be analyzed using the free theory on the EAdS$_2$ classical string dual to the Wilson loop without insertions. When two of the operators have a large charge, $1 \ll J \ll g$, the leading contributions (in $1/J$) come from diagrams in which the light operators are fully contracted with the large charges, and the remaining fields of the large charges are contracted with each other.

noting $J!/(J-\ell_{\text{tot}})! = J^{\ell_{\text{tot}}} + O(J^{\ell_{\text{tot}}-1})$, we find:

$$\frac{\langle\langle Z^J(-\varphi_L)\bar{Z}^J(\varphi_L)\prod_{i=1}^n Z^{\ell_i}(\varphi_i)\prod_{j=1}^m \bar{Z}^{\bar{\ell}_j}(\bar{\varphi}_j)\rangle\rangle}{\langle\langle Z^J(-\varphi_L)\bar{Z}^J(\varphi_L)\rangle\rangle}$$
$$= g^{\ell_{\text{tot}}}\left(J^{\ell_{\text{tot}}}\frac{\left(\frac{4}{\pi}\right)^{\ell_{\text{tot}}} d^{2\ell_{\text{tot}}}}{\prod_{i=1}^n d(\varphi_L,\varphi_i)^{2\ell_i}\prod_{j=1}^m d(-\varphi_L,\varphi_j)^{2\ell_j}}\delta_{\ell_{\text{tot}},\bar{\ell}_{\text{tot}}} + O(J^{\ell_{\text{tot}}-1})\right) + O(g^{\ell_{\text{tot}}-1}). \tag{4.63}$$

This matches the leading term in the small $\mathcal{J}$ expansion of eq. (4.43), which is given by replacing $c^2 \to \mathcal{J}/\pi$. One consequence of this comparison is that we may view the light vertex operators on the $\mathcal{J} \ll 1$ semiclassical string as arising from the boundary-to-boundary contractions on the EAdS$_2$ string between the light insertions and the charge $J \gg 1$ insertions. The factors of $c^2 \sim J$ in the vertex operators reflect the fact that there are J fields in the large insertions that the light insertions can contract with.

Large $\mathcal{J}$. When $\mathcal{J} \gg 1$, $\mathcal{J}$ and c^2 are related by the asymptotic series

$$\mathcal{J} = -2\log(1-c^2) + 4(2\log 2 - 1) + O((1-c^2)\log(1-c^2)), \tag{4.64}$$
$$c^2 = 1 - \frac{16}{e^2}e^{-\frac{\mathcal{J}}{2}} + O(\mathcal{J}e^{-\mathcal{J}}). \tag{4.65}$$

We have already noted the leading large $\mathcal{J}$ behavior of the two-point function in eq. (4.42). Meanwhile, the leading behavior of the three-point function is especially simple:

$$\frac{c^2_{J+\ell,J,\ell}}{n_{J+\ell}n_J n_\ell} = g^\ell\left[\frac{\pi^\ell}{\ell!} + O(e^{-\frac{\mathcal{J}}{2}})\right] + O(g^{\ell-1}). \tag{4.66}$$

JHEP03(2022)020

It is perhaps interesting to compare eqs. (4.58) and (4.66) with the general charge dependence of the heavy-heavy-light OPE coefficient that one would expect based on an effective field theory analysis expanding in inverse powers of the large charge. As in [5, 7], the OPE coefficient typically grows as a power of the large charge. Though the extremal OPE coefficient indeed has this behavior at small $\mathcal{J}$ (see eq. (4.55)), we see from eq. (4.66) that it instead saturates to a constant at large $\mathcal{J}$.

Finally, as noted in [38], if $\mathcal{J}$ were the only parameter governing the correlators when $\mathcal{J}$ is large, then the $1 \ll g \ll J$ regime probed by eqs. (4.42) and (4.66) should match the $g \ll 1 \sim J$ regime accessible to weakly coupled gauge theory, thus creating a bridge between two regimes that a priori seem very different. This agreement was verified in [38], at least schematically, for the correlator of the half-BPS Wilson loop and a single large charge insertion off the Wilson loop. Likewise, in [9] the anomalous dimensions of "words" composed of many copies of Z interspersed with orthogonal scalars inserted on the half-BPS Wilson loop were found to match in both the small g, large J regime and the large g, large $\mathcal{J}$ regime. However, we observe that this agreement between the two regimes does not extend to the correlators we have been studying. From either localization [12] or gauge theory [19], one finds that the two and three-point functions in the weakly coupled limit are

$$\langle\langle \tilde{\Phi}^J \tilde{\Phi}^J \rangle\rangle = (-g^2)^J \left(1 - \frac{2\pi^2}{3} g^2 + O(g^4)\right), \tag{4.67}$$

$$\frac{c^2_{J+\ell,J,\ell}}{n_{J+\ell} n_J n_\ell} = 1 + \frac{2\pi^2 g^2}{3} + O(g^4). \tag{4.68}$$

These are manifestly different from eqs. (4.42) and (4.66).

Acknowledgments

We are grateful to Nadav Drukker for useful correspondence. The work of SG and BO is supported in part by the US NSF under Grant No. PHY-1914860.

A Derivative of the quasi-momentum

In this appendix, we derive the expression for the derivative of the quasi-momentum, eq. (3.34).

For this purpose, we use the fact that the one form $p_{\rm cl} du$ has poles with residue J at $x = 0$ and $x = \infty$, while its integral along two branch cuts gives $-J$. From these properties, we immediately conclude that its derivative $\partial_J p_{\rm cl} du$ satisfies

1. $\oint_{\mathcal{C}_\pm} \partial_J p_{\rm cl} du = -1$.
2. $\oint_{x=0} \partial_J p_{\rm cl} du = \oint_{x=\infty} \partial_J p_{\rm cl} du = 1$.

In addition, one can check that $p_{\rm cl} du$ flips a sign upon $x \to -x^{-1}$. This follows from the definition of the (quantum) quasi-momentum, eq. (3.23).

JHEP03(2022)020

These conditions are sufficient for fixing the one form up to a constant α:

$$\partial_J p_{\rm cl} du = \frac{(x + x^{-1} + \alpha)dx}{\sqrt{(x - e^{i\theta_0})(x - e^{-i\theta_0})(x + e^{i\theta_0})(x + e^{-i\theta_0})}}\,. \tag{A.1}$$

To determine α, we expand the quantum quasi-momentum eq. (3.23) around $x = 0$:

$$p(x)du \sim \frac{J}{x}dx + \sum_{k=1}^{J}(x_k - x_k^{-1})dx + \mathcal{O}(x)\,. \tag{A.2}$$

In the classical limit, x_k's are distributed symmetrically with respect to the real axis (see figure 2), we have

$$\sum_{k=1}^{J}(x_k - x_k^{-1}) \overset{J\to\infty}{=} 0\,. \tag{A.3}$$

Comparing this with the expansion of eq. (A.1) around $x = 0$, one can show that $\alpha = 0$ and reproduce eq. (3.34).

B Supersymmetries of the classical string

This appendix demonstrates that the string solution identified in eq. (4.7) has the same supersymmetries as the string solution analyzed in [9], which corresponds to $c = 1$, and therefore has the same supersymmetries as the Wilson operator with Z^J and $\bar{Z}^J$ inserted. More precisely, we will impose the supersymmetry conditions identified in section 4.2 of [9] on a string ansatz and will show that eq. (4.7) give the general solution to the resulting pair of differential equations. We closely follow the approach of [9]. To avoid confusion, it should be noted that some of the notation in this appendix differs from that in the rest of the text.

Letting κ, λ denote the spacetime indices on $\mathrm{AdS}_5 \times S^5$ and run over $t, \rho, \theta, \phi, \ldots$, and letting $X^\kappa = (\rho, t, \theta, \phi, \ldots)$, the relevant part of the metric is

$$ds^2 = G_{\kappa\lambda}dX^\kappa dX^\lambda = -\cosh^2\rho dt^2 + d\rho^2 + d\theta^2 + \sin^2\theta d\phi^2. \tag{B.1}$$

We introduce the vielbeins $e^a = e^a{}_\kappa dX^\kappa$ satisfying $ds^2 = \eta_{ab}e^a e^b$ where $\eta_{ab} = \mathrm{diag}(-1, 1, \ldots, 1)$ and $a = 0, 1, 2 \ldots, 9$. The relevant vielbeins are $e^0 = \cosh\rho dt$, $e^1 = d\rho$, $e^5 = d\theta$, and $e^6 = \sin\theta d\phi$. We introduce 32×32 real constant Dirac matrices Γ_a on 10 dimensional Minkowski space; they satisfy the Clifford algebra $\{\Gamma_a, \Gamma_b\} = 2\eta_{ab}$. The Dirac matrices on $\mathrm{AdS}_5 \times S^5$ are then $\gamma_\kappa \equiv e^a{}_\kappa \Gamma_a$, and satisfy $\{\gamma_\kappa, \gamma_\lambda\} = 2G_{\kappa\lambda}$. The relevant γ matrices are $\gamma_t = \cosh\rho\Gamma_0$, $\gamma_\rho = \Gamma_1$, $\gamma_\theta = \Gamma_5$, and $\gamma_\phi = \sin\theta\Gamma_6$. Finally, we define the chirality matrix $\Gamma_\star = \Gamma_0\Gamma_1\Gamma_2\Gamma_3\Gamma_4$, which satisfies $[\Gamma_\star, \Gamma_a] = 0$ for $a = 0, \ldots, 4$, $\{\Gamma_\star, \Gamma_b\} = 0$ for $b = 5, \ldots, 9$, and $\Gamma_\star^2 = -1$.

The supersymmetries of a string $X^\kappa(\sigma, \tau)$ embedded in $\mathrm{AdS}_5 \times S^5$, with σ and τ as worldsheet coordinates, are determined by the linearly independent solutions to the Killing spinor equation,

$$(D_\kappa + \frac{i}{2}\Gamma_\star\gamma_\kappa)\epsilon = 0, \tag{B.2}$$

JHEP03(2022)020

that also satisfy the projection condition imposing kappa symmetry, $\Gamma\epsilon = \epsilon$. Here, $D_\kappa \equiv \partial_\kappa + \frac{1}{4}\omega_\kappa^{ab}\Gamma_{ab}$ is the spinor covariant derivative and the relevant components of the spin connection are $\omega_t^{01} = \sinh\rho$ and $\omega_\phi^{56} = -\cos\theta$. Further, the kappa symmetry projector is

$$\Gamma \equiv \frac{1}{\sqrt{-h}}\partial_\tau x^\kappa \partial_\sigma x^\lambda \gamma_\kappa \gamma_\lambda K, \tag{B.3}$$

where h is the metric induced on the string worldsheet and K acts by complex conjugation to the right. As noted in [9], the general t, ρ, θ, ϕ dependence of the Killing spinors may be written

$$\epsilon = e^{-\frac{i}{2}(\rho\Gamma_\star\Gamma_1 + \theta\Gamma_\star\Gamma_5)} e^{-\frac{i}{2}(t\Gamma_\star\Gamma_0 + i\phi\Gamma_5\Gamma_6)}\epsilon_0, \tag{B.4}$$

where ϵ_0 does not depend on the relevant coordinates.

Finally, let us consider the string ansatz of section 4.1 of [9]: $t = \omega\tau$, $\phi = w_1\tau$, $\rho = \rho(\sigma)$, $\theta = \theta(\sigma)$. When $w_1 = \omega$ and $\sin\theta = \operatorname{sech}\rho = \tanh(\omega\sigma)$, [9] showed that imposing the projection condition on eq. (B.4) reduces to two compatible conditions on ϵ_0:

$$(\Gamma_\star\Gamma_0\Gamma_5\Gamma_6 - i)\epsilon_0 = 0, \tag{B.5}$$

$$(\Gamma_0\Gamma_1 K + 1)\epsilon_0 = 0. \tag{B.6}$$

These each halve the degrees of freedom of ϵ_0 and imply that the string solution, like the dual half-BPS Wilson operator with Z^J and $\bar{Z}^J$ inserted, is quarter-BPS. We now derive a more general string configuration, specified by $\theta(\sigma)$ and $\rho(\sigma)$, with these supersymmetries.

To begin, the metric induced on the worldsheet is

$$h_{\alpha\beta}d\sigma^\alpha d\sigma^\beta = (-\omega^2\cosh^2\rho + \sin^2\theta w_1^2)d\tau^2 + ((\rho')^2 + (\theta')^2)d\sigma^2, \tag{B.7}$$

where the prime denotes differentiation with respect to σ, and the projector becomes

$$\Gamma = \frac{\omega\rho'\cosh\rho\Gamma_0\Gamma_1 + \omega\theta'\cosh\rho\Gamma_0\Gamma_5 + w_1\rho'\sin\theta\Gamma_6\Gamma_1 + w_1\theta'\sin\theta\Gamma_6\Gamma_5}{\sqrt{(\omega^2\cosh^2\rho - w_1^2\sin^2\theta)((\rho')^2 + (\theta')^2)}}K. \tag{B.8}$$

Γ is a function only of σ, and the τ dependence of ϵ is contained in the right exponent in eq. (B.4). Thus, for $\Gamma\epsilon = \epsilon$ to hold for all τ, we follow [9] and impose[33]

$$(\omega\Gamma_\star\Gamma_0 + iw_1\Gamma_5\Gamma_6)\epsilon_0 = 0. \tag{B.9}$$

Acting on the left of the above condition with $-i\Gamma_\star\Gamma_0$, we see that eq. (B.9) is equivalent to eq. (B.5) only if $w_1 = \omega$, as in the Drukker-Kawamoto solution.

More non-trivially, to get the analog of eq. (B.6), we commute Γ past $e^{-\frac{i}{2}(\rho\Gamma_\star\Gamma_1 + \theta\Gamma_\star\Gamma_5)}$ in $\Gamma\epsilon = \epsilon$ and arrive at

$$\frac{(\omega\rho'\cosh\rho\cos\theta - \omega\theta'\sin\theta\sinh\rho)\Gamma_0\Gamma_1 + (\omega\theta'\cosh\rho\cos\theta + \omega\rho'\sin\theta\sinh\rho)\Gamma_0\Gamma_5}{\sqrt{(\omega^2\cosh^2\rho - w_1^2\sin^2\theta)((\rho')^2 + (\theta')^2)}}K\epsilon_0 = \epsilon_0. \tag{B.10}$$

[33] One could try to impose more generally that $(\omega\Gamma_\star\Gamma_0 + iw_1\Gamma_5\Gamma_6)\epsilon_0 = \lambda\epsilon_0$ for some complex λ. Then, because of the action of K in Γ, λ must be imaginary in order for $\Gamma\epsilon = \epsilon$ to hold for all τ. But since $\Gamma_\star\Gamma_0$ and $\Gamma_5\Gamma_6$ can be simultaneously diagonalized (because they commute) and have eigenvalues ± 1 and $\pm i$, respectively, λ must also be real. Therefore, $\lambda = 0$.

JHEP03(2022)020

In order for eq. (B.10) to be equivalent to eq. (B.6), θ and ρ must satisfy the following two differential equations.

$$\theta' \cosh\rho\cos\theta + \rho' \sin\theta \sinh\rho = 0, \qquad \frac{\rho' \cosh\rho\cos\theta - \theta' \sin\theta\sinh\rho}{\sqrt{(\cosh^2\rho - \sin^2\theta)((\rho')^2 + (\theta')^2)}} = -1, \tag{B.11}$$

where we have assumed $\omega > 0$. The first equation is separable and its general solution is

$$\sin\theta = \frac{c}{\cosh\rho}. \tag{B.12}$$

Since $\theta \in [0, \pi]$, it follows that $0 \leq c \leq 1$. The second differential equation is then automatically satisfied. Thus, along with $t = \phi = \omega\tau$, eq. (B.12) defines the more general string configuration with the supersymmetries specified by eqs. (B.5) and (B.6).

References

[1] D.E. Berenstein, J.M. Maldacena and H.S. Nastase, *Strings in flat space and pp waves from $N = 4$ superYang-Mills*, *JHEP* **04** (2002) 013 [hep-th/0202021] [INSPIRE].

[2] S.S. Gubser, I.R. Klebanov and A.M. Polyakov, *A Semiclassical limit of the gauge/string correspondence*, *Nucl. Phys. B* **636** (2002) 99 [hep-th/0204051] [INSPIRE].

[3] N. Beisert et al., *Review of AdS/CFT Integrability: An Overview*, *Lett. Math. Phys.* **99** (2012) 3 [arXiv:1012.3982] [INSPIRE].

[4] S. Hellerman, D. Orlando, S. Reffert and M. Watanabe, *On the CFT Operator Spectrum at Large Global Charge*, *JHEP* **12** (2015) 071 [arXiv:1505.01537] [INSPIRE].

[5] A. Monin, D. Pirtskhalava, R. Rattazzi and F.K. Seibold, *Semiclassics, Goldstone Bosons and CFT data*, *JHEP* **06** (2017) 011 [arXiv:1611.02912] [INSPIRE].

[6] L. Álvarez-Gaumé, O. Loukas, D. Orlando and S. Reffert, *Compensating strong coupling with large charge*, *JHEP* **04** (2017) 059 [arXiv:1610.04495] [INSPIRE].

[7] D. Jafferis, B. Mukhametzhanov and A. Zhiboedov, *Conformal Bootstrap At Large Charge*, *JHEP* **05** (2018) 043 [arXiv:1710.11161] [INSPIRE].

[8] L.A. Gaumé, D. Orlando and S. Reffert, *Selected topics in the large quantum number expansion*, *Phys. Rept.* **933** (2021) 2180 [arXiv:2008.03308] [INSPIRE].

[9] N. Drukker and S. Kawamoto, *Small deformations of supersymmetric Wilson loops and open spin-chains*, *JHEP* **07** (2006) 024 [hep-th/0604124] [INSPIRE].

[10] S. Giombi, R. Roiban and A.A. Tseytlin, *Half-BPS Wilson loop and AdS_2/CFT_1*, *Nucl. Phys. B* **922** (2017) 499 [arXiv:1706.00756] [INSPIRE].

[11] S. Giombi, J. Jiang and S. Komatsu, *Giant Wilson loops and $AdS_2/dCFT_1$*, *JHEP* **11** (2020) 064 [arXiv:2005.08890] [INSPIRE].

[12] S. Giombi and S. Komatsu, *Exact Correlators on the Wilson Loop in $\mathcal{N} = 4$ SYM: Localization, Defect CFT, and Integrability*, *JHEP* **05** (2018) 109 [*Erratum ibid.* **11** (2018) 123] [arXiv:1802.05201] [INSPIRE].

JHEP03(2022)020

[13] S. Giombi and S. Komatsu, *More Exact Results in the Wilson Loop Defect CFT: Bulk-Defect OPE, Nonplanar Corrections and Quantum Spectral Curve*, *J. Phys. A* **52** (2019) 125401 [arXiv:1811.02369] [INSPIRE].

[14] P. Liendo, C. Meneghelli and V. Mitev, *Bootstrapping the half-BPS line defect*, *JHEP* **10** (2018) 077 [arXiv:1806.01862] [INSPIRE].

[15] P. Ferrero and C. Meneghelli, *Bootstrapping the half-BPS line defect CFT in $N = 4$ supersymmetric Yang-Mills theory at strong coupling*, *Phys. Rev. D* **104** (2021) L081703 [arXiv:2103.10440] [INSPIRE].

[16] J. Barrat, A. Gimenez-Grau and P. Liendo, *Bootstrapping holographic defect correlators in $\mathcal{N} = 4$ super Yang-Mills*, arXiv:2108.13432 [INSPIRE].

[17] N. Drukker, *Integrable Wilson loops*, *JHEP* **10** (2013) 135 [arXiv:1203.1617] [INSPIRE].

[18] D. Correa, J. Henn, J. Maldacena and A. Sever, *An exact formula for the radiation of a moving quark in $N = 4$ super Yang-Mills*, *JHEP* **06** (2012) 048 [arXiv:1202.4455] [INSPIRE].

[19] N. Kiryu and S. Komatsu, *Correlation Functions on the Half-BPS Wilson Loop: Perturbation and Hexagonalization*, *JHEP* **02** (2019) 090 [arXiv:1812.04593] [INSPIRE].

[20] D. Grabner, N. Gromov and J. Julius, *Excited States of One-Dimensional Defect CFTs from the Quantum Spectral Curve*, *JHEP* **07** (2020) 042 [arXiv:2001.11039] [INSPIRE].

[21] A. Cavaglià, N. Gromov, J. Julius and M. Preti, *Integrability and conformal bootstrap: One dimensional defect conformal field theory*, *Phys. Rev. D* **105** (2022) L021902 [arXiv:2107.08510] [INSPIRE].

[22] J. Polchinski and J. Sully, *Wilson Loop Renormalization Group Flows*, *JHEP* **10** (2011) 059 [arXiv:1104.5077] [INSPIRE].

[23] M. Beccaria, S. Giombi and A. Tseytlin, *Non-supersymmetric Wilson loop in $\mathcal{N} = 4$ SYM and defect* 1*d CFT*, *JHEP* **03** (2018) 131 [arXiv:1712.06874] [INSPIRE].

[24] M. Beccaria, S. Giombi and A.A. Tseytlin, *Correlators on non-supersymmetric Wilson line in $\mathcal{N} = 4$ SYM and AdS_2/CFT_1*, *JHEP* **05** (2019) 122 [arXiv:1903.04365] [INSPIRE].

[25] D.H. Correa, V.I. Giraldo-Rivera and G.A. Silva, *Supersymmetric mixed boundary conditions in AdS_2 and $DCFT_1$ marginal deformations*, *JHEP* **03** (2020) 010 [arXiv:1910.04225] [INSPIRE].

[26] G. Cuomo, Z. Komargodski and A. Raviv-Moshe, *Renormalization Group Flows on Line Defects*, *Phys. Rev. Lett.* **128** (2022) 021603 [arXiv:2108.01117] [INSPIRE].

[27] M. Beccaria, S. Giombi and A.A. Tseytlin, *Higher order RG flow on the Wilson line in $\mathcal{N} = 4$ SYM*, *JHEP* **01** (2022) 056 [arXiv:2110.04212] [INSPIRE].

[28] N. Gromov and A. Sever, *Analytic Solution of Bremsstrahlung TBA*, *JHEP* **11** (2012) 075 [arXiv:1207.5489] [INSPIRE].

[29] S. Giombi, S. Komatsu and B. Offertaler, *Large Charges on the Wilson loop in $\mathcal{N} = 4$ SYM II*, in preparation.

[30] A. Miwa and T. Yoneya, *Holography of Wilson-loop expectation values with local operator insertions*, *JHEP* **12** (2006) 060 [hep-th/0609007] [INSPIRE].

[31] N. Drukker, D.J. Gross and H. Ooguri, *Wilson loops and minimal surfaces*, *Phys. Rev. D* **60** (1999) 125006 [hep-th/9904191] [INSPIRE].

JHEP03(2022)020

[32] P. Yang, Y. Jiang, S. Komatsu and J.-B. Wu, *D-branes and Orbit Average*, *SciPost Phys.* **12** (2022) 055 [arXiv:2103.16580] [INSPIRE].

[33] Z. Bajnok, R.A. Janik and A. Wereszczyński, *HHL correlators, orbit averaging and form factors*, *JHEP* **09** (2014) 050 [arXiv:1404.4556] [INSPIRE].

[34] A. Grassi, Z. Komargodski and L. Tizzano, *Extremal correlators and random matrix theory*, *JHEP* **04** (2021) 214 [arXiv:1908.10306] [INSPIRE].

[35] M. Beccaria, F. Galvagno and A. Hasan, $\mathcal{N} = 2$ *conformal gauge theories at large R-charge: the* SU(N) *case*, *JHEP* **03** (2020) 160 [arXiv:2001.06645] [INSPIRE].

[36] N. Gromov, S. Schäfer-Nameki and P. Vieira, *Efficient precision quantization in AdS/CFT*, *JHEP* **12** (2008) 013 [arXiv:0807.4752] [INSPIRE].

[37] B. Vicedo, *Semiclassical Quantisation of Finite-Gap Strings*, *JHEP* **06** (2008) 086 [arXiv:0803.1605] [INSPIRE].

[38] K. Zarembo, *Open string fluctuations in* $AdS_5 \times S^5$ *and operators with large R charge*, *Phys. Rev. D* **66** (2002) 105021 [hep-th/0209095] [INSPIRE].

[39] S. Giombi and V. Pestun, *Correlators of local operators and* 1/8 *BPS Wilson loops on* S^2 *from* 2*d YM and matrix models*, *JHEP* **10** (2010) 033 [arXiv:0906.1572] [INSPIRE].

[40] S. Giombi and V. Pestun, *Correlators of Wilson Loops and Local Operators from Multi-Matrix Models and Strings in AdS*, *JHEP* **01** (2013) 101 [arXiv:1207.7083] [INSPIRE].

[41] N. Drukker, S. Giombi, R. Ricci and D. Trancanelli, *More supersymmetric Wilson loops*, *Phys. Rev. D* **76** (2007) 107703 [arXiv:0704.2237] [INSPIRE].

[42] N. Drukker, S. Giombi, R. Ricci and D. Trancanelli, *Wilson loops: From four-dimensional SYM to two-dimensional YM*, *Phys. Rev. D* **77** (2008) 047901 [arXiv:0707.2699] [INSPIRE].

[43] N. Drukker, S. Giombi, R. Ricci and D. Trancanelli, *Supersymmetric Wilson loops on* S^3, *JHEP* **05** (2008) 017 [arXiv:0711.3226] [INSPIRE].

[44] S. Hellerman and S. Maeda, *On the Large R-charge Expansion in* $\mathcal{N} = 2$ *Superconformal Field Theories*, *JHEP* **12** (2017) 135 [arXiv:1710.07336] [INSPIRE].

[45] J.K. Erickson, G.W. Semenoff and K. Zarembo, *Wilson loops in* $N = 4$ *supersymmetric Yang-Mills theory*, *Nucl. Phys. B* **582** (2000) 155 [hep-th/0003055] [INSPIRE].

[46] N. Drukker and D.J. Gross, *An Exact prediction of* $N = 4$ *SUSYM theory for string theory*, *J. Math. Phys.* **42** (2001) 2896 [hep-th/0010274] [INSPIRE].

[47] V. Pestun, *Localization of gauge theory on a four-sphere and supersymmetric Wilson loops*, *Commun. Math. Phys.* **313** (2012) 71 [arXiv:0712.2824] [INSPIRE].

[48] M. Cooke, A. Dekel and N. Drukker, *The Wilson loop CFT: Insertion dimensions and structure constants from wavy lines*, *J. Phys. A* **50** (2017) 335401 [arXiv:1703.03812] [INSPIRE].

[49] M. Kim, N. Kiryu, S. Komatsu and T. Nishimura, *Structure Constants of Defect Changing Operators on the* 1/2 *BPS Wilson Loop*, *JHEP* **12** (2017) 055 [arXiv:1710.07325] [INSPIRE].

[50] J. Qiao and S. Rychkov, *A tauberian theorem for the conformal bootstrap*, *JHEP* **12** (2017) 119 [arXiv:1709.00008] [INSPIRE].

[51] V.A. Kazakov, A. Marshakov, J.A. Minahan and K. Zarembo, *Classical/quantum integrability in AdS/CFT*, *JHEP* **05** (2004) 024 [hep-th/0402207] [INSPIRE].

JHEP03(2022)020

[52] N. Dorey and B. Vicedo, *On the dynamics of finite-gap solutions in classical string theory*, *JHEP* **07** (2006) 014 [hep-th/0601194] [INSPIRE].

[53] B. Eynard, *A short overview of the "Topological recursion"*, arXiv:1412.3286 [INSPIRE].

[54] B. Eynard and N. Orantin, *Invariants of algebraic curves and topological expansion*, *Commun. Num. Theor. Phys.* **1** (2007) 347 [math-ph/0702045] [INSPIRE].

[55] G. Sizov and S. Valatka, *Algebraic Curve for a Cusped Wilson Line*, *JHEP* **05** (2014) 149 [arXiv:1306.2527] [INSPIRE].

[56] J.M. Maldacena, *Wilson loops in large N field theories*, *Phys. Rev. Lett.* **80** (1998) 4859 [hep-th/9803002] [INSPIRE].

[57] S.-J. Rey and J.-T. Yee, *Macroscopic strings as heavy quarks in large N gauge theory and anti-de Sitter supergravity*, *Eur. Phys. J. C* **22** (2001) 379 [hep-th/9803001] [INSPIRE].

[58] N. Drukker, 1/4 *BPS circular loops, unstable world-sheet instantons and the matrix model*, *JHEP* **09** (2006) 004 [hep-th/0605151] [INSPIRE].

[59] T. Enari and A. Miwa, *Semi-classical correlator for* 1/4 *BPS Wilson loop and chiral primary operator with large R-charge*, *Phys. Rev. D* **86** (2012) 106004 [arXiv:1208.0821] [INSPIRE].

[60] F.A. Dolan and H. Osborn, *Conformal Partial Waves: Further Mathematical Results*, arXiv:1108.6194 [INSPIRE].

[61] N.M. Temme, *Large parameter cases of the Gauss hypergeometric function*, *J. Comput. Appl. Math.* **153** (2003) 441.

JHEP03(2022)020